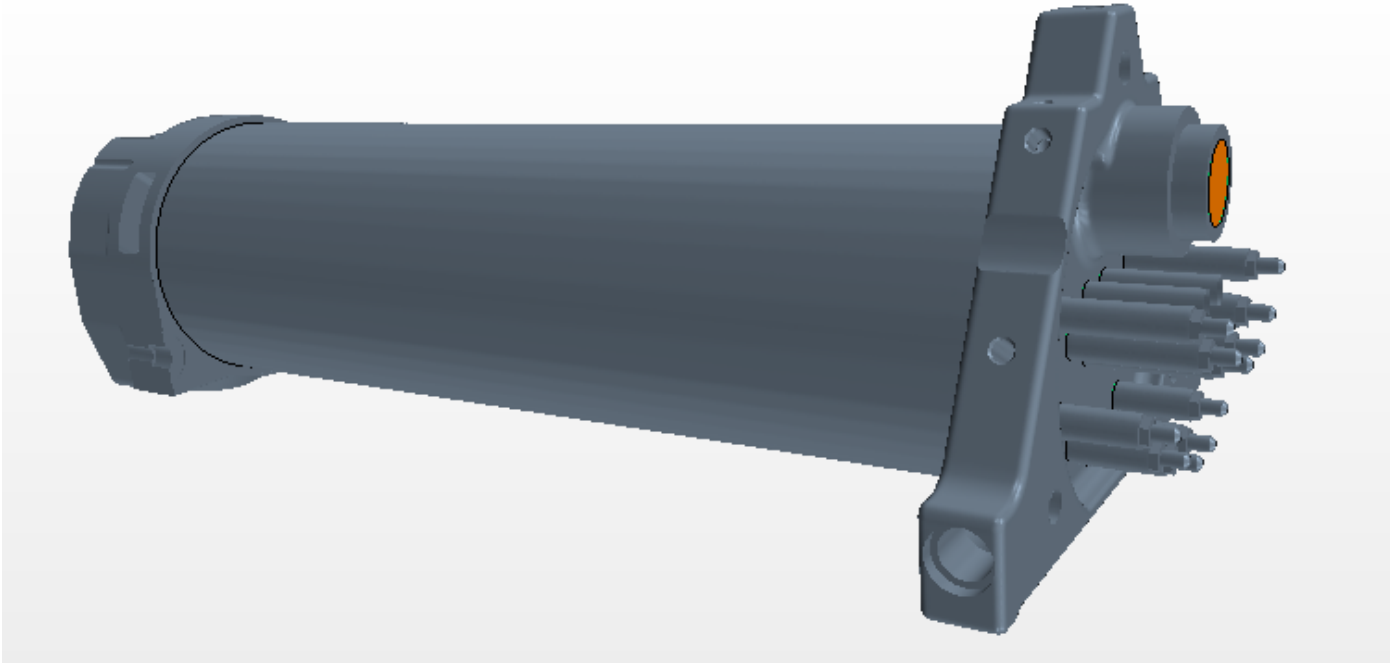




**CHALMERS**  
UNIVERSITY OF TECHNOLOGY

---



# Simulation of heating systems in vehicles

Master's thesis in automotive engineering

Mohamed Tarig Mohamed

---

Division of Fluid Dynamics  
Department of Applied Mechanics  
CHALMERS UNIVERSITY OF TECHNOLOGY  
Gothenburg, Sweden 2015





MASTER'S THESIS IN AUTOMOTIVE ENGINEERING

# Simulation of heating systems in vehicles

Mohamed Tarig Mohamed

Department of Applied Mechanics  
Division of Fluid Dynamics  
CHALMERS UNIVERSITY OF TECHNOLOGY  
Göteborg, Sweden 2015

Simulation of heating systems in vehicles

Mohamed Tarig Mohamed

© Mohamed Tarig Mohamed, 2015-11-14

Master's Thesis 2015:89

ISSN 1652-8557

Department of Applied Mechanics

Division of Fluid Dynamics

Chalmers University of Technology

SE-412 96 Göteborg

Sweden

Telephone: + 46 (0) 31-772 1000

Cover:

Heating unit that is used in the vehicle heating system

Name of the printers / Department of Applied Mechanics

Göteborg, Sweden 2015-11-14

Simulation of heating systems in vehicles  
Master's thesis in Master's automotive engineering  
Mohamed Tarig Mohamed  
Department of Applied Mechanics  
Division of Fluid Dynamics  
Chalmers University of Technology

## **Abstract**

Vehtec AB is a company working on building and developing heating systems for buses. One of the main components of the heating system is the heating unit, which called Eldi heater.

The purpose of the thesis is to simulate Eldi heater using commercial CFD software, and to validate the simulation results by running a lap experiment. This simulation will provide an inner view of the flow motion and what could be done to improve the efficiency of the heater.

After running the first simulation for the original model, it seemed likely that the efficiency could be improved by altering the geometry. Three models with different geometry were built and simulated to try to improve the flow turbulence and the duration the water spend inside the heating unit, hence increasing the heat transfer rate from the heating elements to the water volume.

Two models have showed improvement compared to the original one. Model two had the best results with temperature increase by 7% and 14 % reduction in time.

Key words:

Eldi pre-heater, Vehtec, STAR CCM+, heating unit, CFD simulation, vehicle heating.



# Contents

Abstract .....	IV
Contents .....	VI
Preface.....	VIII
Notations .....	IX
1 Introduction.....	1
1.1 Background:.....	1
1.2 Aim of the work: .....	1
1.3 Limitation.....	2
1.4 What is CFD?.....	2
1.5 How does a CFD code work? .....	3
1.5.1 Pre-processor.....	3
1.5.2 Solvers.....	3
1.5.3 Post-processor .....	4
2 Modeling in STAR-CCM+ .....	5
2.1 Modeling geometry .....	5
2.2 Defining the simulation topology .....	5
2.3 Surface repair .....	5
2.4 Meshing.....	8
2.4.1 Surface mesher models .....	9
2.4.2 Volume mesher .....	10
2.5 Modeling physics .....	13
2.5.1 Space models .....	13
2.5.2 Time models.....	13
2.5.3 Modelling materials .....	14
2.5.4 Modelling flow and energy .....	14
2.5.5 Modelling the viscous regime .....	14
2.5.6 Modelling wall treatment.....	15
3 The Experiment.....	16
4 Modelling and Results .....	18
4.1 Geometry.....	18
4.2 Boundary conditions .....	18
4.3 Mesh refinement .....	19
4.4 Modelling.....	22
4.4.1 Building the geometry.....	22

4.4.2	Generating the mesh .....	22
4.4.3	Physics continua.....	22
4.4.4	Residuals and mass imbalance.....	23
4.5	Results.....	23
4.5.1	The original model.....	23
4.5.2	Model 1 .....	27
4.5.3	Model 2 .....	29
4.5.4	Model 3 .....	31
4.5.5	Model 4 .....	33
5	Discussion and conclusion.....	35
6	References.....	36
7	Appendix.....	37
7.1	Photos from the experiment.....	37
7.2	Mesh refinement study.....	38
7.3	Simulations results .....	43

## **Preface**

In this study, simulation of heating systems in vehicles has been done using the commercial software STAR CCM+. The work has been carried out from January 2015 to September 2015. The work is apart from the development of the heating system that Vehtec AB is producing. The project is carried out at Vehtec AB and the experiment part is done at Eldi in Stockholm.

Doing this project helped to enhance the knowledge about the Eldi pre heater efficiency and how it could be improved.

I would like to thank Daniel Keiser and Bengt Lindgren for their co-operation and involvement.

Last but not least, I would like to thank my family for being always there to support and encourage me no matter what. Without them, I would not manage to achieve any of my goals.

Göteborg October 2015-11-14

Mohamed Tarig Mohamed

## Notations

CFD	Computational fluid dynamics
CAD	Computational aided design
W	Watt
l/min	liter per minute
mm	millimeter



# 1 Introduction

This chapter will provide a brief description of the project, the goal and the limitations. Additionally, a short description for the CFD software will be written.

## 1.1 Background:

Vehtec AB is a company that has been working with the bus industry for almost two decades. In the past decade, the company's focus has been to increase in-house product development for the heating of buses with sustainability in mind. Vehtec has developed Veheat, which is a patent pending product that is a combination of a radiator and convector of aluminum. This reduced the number of mixed materials and the environmental impact, especially fuel consumption. With increased competition on the market, the need to develop the product further became an apparent issue. By using computer simulation models the product can be evaluated and developed with lower cost and time compared to laboratory testing.

The Figure below shows the heating system inside the vehicle with all its parts and components. The system uses the hot water from the engine to warm the passengers compartment, but in a cold environment the engine needs time to warm up and hence warming the water in the system. As a solution for this problem, an electrical pre-heater is installed to warm the water in the system, hence warming the passengers compartment.

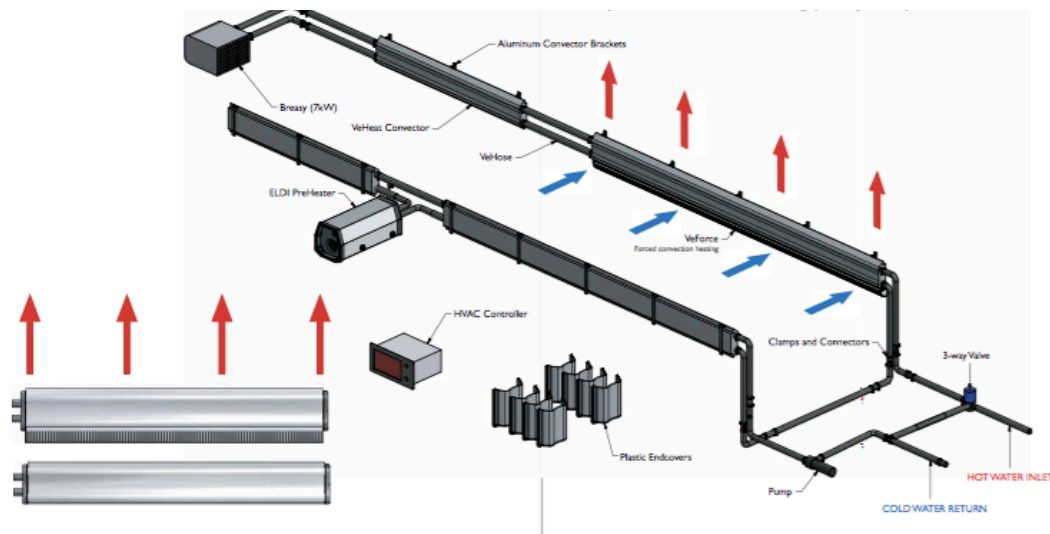


Figure 1 Heating system in vehicles, taken from Vehtec catalogue

## 1.2 Aim of the work:

The aim of the thesis is to design a computational fluid dynamic simulation model, in order to observe the effectiveness of various geometries on the Eldi pre heater.

## 1.3 Limitation

Due to computational resource and time limitations, the modeling will be limited to some criteria. Among the different models that are used for CFD, the modeling in this thesis will be limited to Reynold averaging Navier-Stokes (RANS) model. Regarding the turbulence modeling the model used is the two-equation model ( $K - \epsilon$ ) with wall function. There will be no comparison between different models, due to time limitations. In addition, the simulations will be limited to steady state, the boundary conditions are kept the same for all models and the number of cell is limited to 3 million. If more than 3 million cells are used in the simulation, the simulation will take more than a week to converge, which is not suitable for the thesis time frame.

## 1.4 What is CFD?

CFD stands for computational fluid dynamics, which is a power full tool for simulating fluid turbulence, chemical reactions, heat transfer and many other phenomena related to the fluid flow. In addition, CFD can be defined as a method of applying the laws of fluid mechanics and the mathematical equations and principles to sophisticated computer algorithms to produce software or computer programs for visualizing the data. Alternatively, it is the analysis of fluid flow, heat transfer, and other related phenomena with the aid of advanced physical models, numerical techniques, software and computers.

CFD simulations are used in a wide range of industrial and non-industrial applications, such as:

- Vehicle industry: CFD methods are applied to many areas in vehicle industry, for example to predict the drag and lift forces, simulating the combustion in the combustion chamber, simulating the air flow around the radiator to predict the cooling efficiency and many other applications. CFD has become a vital tool when designing a modern vehicle.
- Cooling of equipment, including microcircuit.

CFD has lagged other CAE (Computer aided engineering) software, because of the complexity of the associated phenomenon in the fluid flow. The final goal from developing CFD software is to reach a tool that is capable to provide a simulation comparable to other CAE tools such as stress analysis codes.

CFD has many advantages compared to testing in the lab, some of this advantages are:

- CFD provides a lower cost compared to running an experiment in a lab or using a wind tunnel in case of running an aerodynamic analysis for a vehicle.
- Short lead-time, by using new software one can prepare and run a simulation in hours.
- A great advantage in CFD is post-processing, which makes understanding the flow features much easier for the user.
- The ability to observe results where experiments cannot be held, such as observing the airflow under the vehicle hood.
- Easy to run different configurations and comparing between them.

One can mention that, CFD has some disadvantages, which is requiring modeling that brings uncertainties and complex phenomena to describe mathematically.  
Versteeg, H.K., Malalasekera, W. (2007).

## 1.5 How does a CFD code work?

All CFD codes use numerical algorithms to solve fluid flows problems. CFD software provides a user interface for the user to input all the problem parameter, boundary conditions and to examine the results of the simulation. Hence, all CFD commercial software is divided into three main categories: pre-processor, solver and post-processor.

### 1.5.1 Pre-processor

Using a user-friendly interface uses the pre-processing to input the case's data into the CFD software. Then the data is transformed into a suitable form for the solver to work on it. In the pre-processing, the user does the following steps:

- Define the geometry of the case, which called the computational domain.
- Define the boundary conditions.
- Create the mesh and choose between different types of meshes that can be used, the selection depends on the case. A suitable mesh for this case might not be a suitable for another case.
- Select the physical models.
- Define the fluid properties.

The solution domain is divided into smaller domains where each one has a center point called a "node". The solution parameters such as pressure, velocity and temperature are saved at the nodes. A general rule is the larger the number of nodes the more accurate the solution. Although by increasing the number of nodes, the solution cost increases in terms of more computational power needed as well as more time is needed to get the solution. The best meshes are the ones that are non-uniform: coarse in the areas where there is a little change between the nodes and finer at areas where the change is relatively large. The ultimate CFD software is the one with the capability to generate an automated mesh that is refined automatically in areas where a refined mesh is needed and coarse when a coarse mesh is needed. The mesh quality is very important as the solution accuracy depends on it.

### 1.5.2 Solvers

The solver uses a numerical technique to find the solution. The most popular technique is the finite volume method, because it has the following advantages:

- It is easy to understand and to code.
- All the terms to be approximated have a physical meaning.
- The solution domain is divided into small non-overlapping control volumes and the differential conservation equations are integrated in each control volume.
- At the center of each control volume, there is a node where the variables are saved.
- It can have any kind of mesh, which makes it suitable for all geometry.
- The values on the faces for each node are interpolated from the values of the nearby nodes.

### 1.5.3 Post-processor

The post-processing is the data visualization tools that are used by the user to observe the solution of the case. These include:

- Geometry and mesh display.
- Vector plots such as speed plots.
- Contour plots such as pressure plots.
- Tracking of particles.
- Surface plots.
- Animation of the fluid flow.

In general, one can say the graphics output for the CFD software have improved the understanding of ideas to the non-specialist.

CFD solutions for fluid flows can be as good as the physics models that impeded in the code, but is user dependent to achieve good accuracy. Therefore, the CFD code user should have skills in order to achieve good results from the simulations. There are decisions and choices that have to be made by the user in order to improve the simulation quality and result in solutions that are more accurate. Those decisions could be to solve the flow for turbulent or laminar, two or three dimension, which model should be used for the turbulent flow and many other decisions and choices. For the user to be able to select the most suitable models for each case this require large experience and knowledge about the CFD codes. Versteeg, H.K., Malalasekera, W. (2007).

## 2 Modeling in STAR-CCM+

STAR CCM+ is commercial software used for fluid dynamics simulations developed by a company called CD-adapco.

There are general steps to be followed when doing a simulation on STAR-CCM+, these steps will be explained and detailed in this chapter in a sequential way, starting from the first step to the last one.

### 2.1 Modeling geometry

Most of the simulations in STAR-CCM+ start with creating a 3D model of the case under investigation. This model can be created in any 3D- CAD software and it has to be well prepared, cleaned of all the unnecessary parts. In addition, STAR-CCM+ has its own 3D-CAD tools, where one can build the model from scratch using these tools.

3D-CAD model is a solid model of the case that is need to be investigated and is created in any of the CAD software packages that is available.

The process of creating a 3D-CAD starts with creating a sketch in 2D. Then this sketch can be converted to 3D model by creating a series of operations such as extruding or revolving. One can modify the model even more by drawing new sketches on the available body and add or subtract parts to the model by performing more operations such as sweeps, lofts, revolution and extrusion.

STAR-CCM+ has a tool called 3D-CAD which allows the user to build 3D models from scratch, this tool is specialized to suit the needs of CFD analysis, it also allows the user to make changes to available models in easy and quick way before rerunning the simulation. CD-adapco (2014).

### 2.2 Defining the simulation topology

Geometry parts are used to define the surface of the model that is going to be simulated, but STAR-CCM+ does not work directly on the geometry parts. The domain where the mesh will be generated and transport equations are going to be solved is defined as regions, boundaries and interfaces.

When a model is being imported into STAR-CCM+, there are tools provided to convert the geometry surfaces into regions, boundaries and interfaces. A recommended practice is that, the user should do this step after making all the changes needed to the geometry part before converting the surfaces to regions and boundaries. CD-adapco (2014).

### 2.3 Surface repair

In order for STAR-CCM+ to create a good mesh the surface of the model should be prepared for the meshing operation. The surface preparation is done by using the surface repair tool. The surface repair tool provides a list of thresholds that counts the number of the faults that are presents on the surface. Each one of these thresholds has a distinguishing color. The surface on the model with a specific fault will have the

color of that fault. After identifying the faults on the model, one can use the available tools to fix these faults.

One thing should be mentioned before explaining the surface repair tool is that, when geometry is imported to STAR-CCM+ the surface of this geometry will be divided into triangles, each on of them is called a face.

The thresholds that are available in the surface repair tool:

### 1. Pierced faces.

When two faces intersect, each other are called pierced faces. This error can be fixed by deleting one of the faces. In many cases, deleting one of the faces might cause another error, so one should be careful when fixing this kind of error.

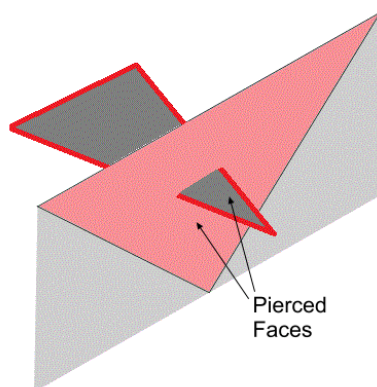


Figure 2 Pierced faces, taken from CD-adapco (2014) manual.

### 2. Face quality.

Face quality is identified as the ratio between the inner circle radius multiplied by 2 and the outer circle radius of the triangle. The face quality ranges between zero and one, zero being the worst quality and one is the ideal quality.

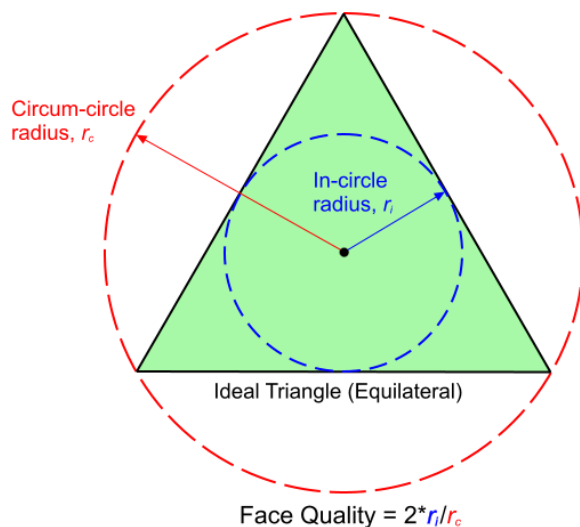


Figure 3 Face quality, taken from CD-adapco (2014) manual.

### 3. Face proximity.

Face proximity is the distance between two faces to the size of the face, it falls between zero and one, the low value indicate fold in the surface. This problem can be fixed by refining the mesh in the area of the fold.

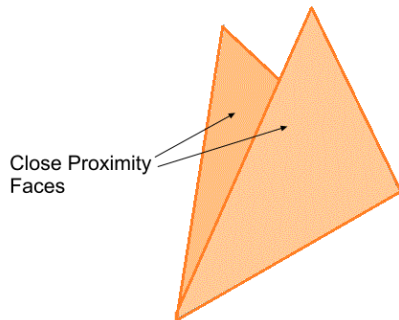


Figure 4 Face proximity, taken from CD-adapco (2014) manual.

### 4. Free edges.

A free edge is an edge that is connected to one face only. This problem can be solved by filling the holes.

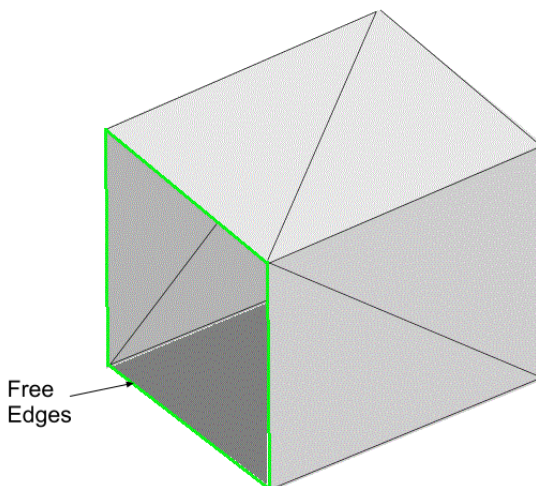


Figure 5 Free edges, taken from CD-adapco (2014) manual.

### 5. Non-manifold edges.

Non-manifold edge is an edge that is connected to more than two faces. This problem can be fixed by deleting one of the extra faces, but one should be careful as deleting a face could cause another error.

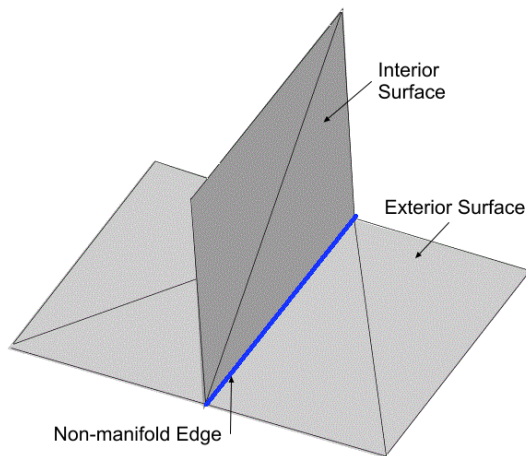


Figure 6 Non manifold edges, taken from CD-adapco (2014) manual.

The above figures shows the error that one should check before start using any one of the repair tools.

Now is time to explain some of the useful tools that one can use to repair the surface.

- Offset faces and edges.

Faces and edges can be inflated or translated in one direction or both directions using this tool. When this tool is activated, the user can specify the surface that should be fixed, the thickness and the direction in which the surface should be inflated or translated.

- Merge and imprint surfaces.

This tool allows the user to merge and imprint two surfaces into each others. This tool is very useful when there are pierced surfaces, these surface can simply be imprinted into each other to become on surface. Also it can be useful when two parts are joined together and they should touching each others at certain surfaces, then these surfaces can be imprinted into each others.

The user can specify a certain tolerance, and if there are two surfaces with a distance between them that is less than the tolerance, these surfaces will be imprinted.

By using the above-mentioned tools, one can prepare the surface for the meshing process, but first one should make sure that all the faults are equal to zero except the face quality, as this one will be fixed when the mesh is been generated. CD-adapco (2014).

## 2.4 Meshing

A mesh is a discretized representation of the computational domain, which the physics solver uses to provide a numerical solution.

The mesh creation in STAR-CCM+ starts with selecting the models for the mesh continua. The mesh models are divided into two main groups, surface mesh and

volume mesh. Each one of these groups has its own models from which the user can choose which suit his simulation purpose the best.

## **2.4.1 Surface mesher models**

The surface remesher is used to improve the quality of the surface by re-triangulate the surface and prepare it for the volume mesh. A golden rule is that, a good volume mesh starts from a good surface mesh.

Two models are available on STAR-CCM+ for the surface remesher.

### **2.4.1.1 Surface remesher:**

The surface remesher has the following properties:

1. Curvature refinement: this option when activated will do a refinement of the surface mesh based on the curvature of the surface.
2. Proximity refinement: when this option is activated, it refines the surface mesh based on the proximity to the original surface.
3. Compatibility refinement: when this option is activated, will do refinement based on the face size during the re-meshing.
4. Retain geometric features: it keeps the feature that is inherited from the original geometry as long as face quality does not reduce.
5. Aligned mesh: when this option is activated, aligned mesh will be generated which means, the rectangular surface will have a uniform size.
6. Base size: here the user can specify the reference length value for all size control.
7. Minimum face quality: the minimum quality to allow topological modification, this value should be between zero and 0.2.
8. Surface growth rate: the maximum ratio between two neighbors triangles.



Figure 7 re-meshed surfaces, taken from CD-adapco (2014) manual.

#### 2.4.1.2 Surface wrapper

The surface wrapper can be used to generate a surface that is manifold, closed and non-intersecting. The surface wrapper is used when poor quality CAD is used. See CD-adapco manual (2014).

### 2.4.2 Volume mesher

STAR-CCM+ provides alternative types of meshes that are available for the user. These volume meshes are used to generate the volume mesh after re-meshing the surface. Each one of these meshes has advantages and disadvantages, depending on the user application and preferences.

The types for the meshing models are:

#### 1. Tetrahedral mesh.

In all types of mesher, the tetrahedral is the fastest mesh generator and uses the least amount of memory. It also provides a multi region mesh and conformal mesh between the different regions.

#### 2. Trimmed mesh.

The trimmed mesh model provides a robust, fast and high quality mesh that is suitable for simple and complex geometry. This type of mesh is suitable for large domains such as car in a wind tunnel, airplanes and ships.

General rules for using trimmed mesh are:

- Simulations where have a large aligned flow directions.
- When refinement in the wake region is needed, for example a car in a wind tunnel.

#### 3. Thin mesh.

Thin mesher is used to generate mesh for thin parts like sheet metals. The type of mesh that is generated by the thin mesher is a prismatic mesh.

#### 4. Advancing layer mesh with built in prismatic layers.

This mesher model generates a prismatic layer mesh around the surface of the region and then fill the region with a polyhedral mesh. When this mesher model is used there is no need to use a separate prismatic mesher model as it is included in the mesher model already.

## 5. Prism layer mesher

The prism layer mesher is used to generate the mesh around the surface; it has to be used with a core volume mesh, as it does not generate the mesh in the core. The prism layers can only be generated at the boundary of type wall.

The importance of the prism layers generated from its ability to help resolve the wall flow accurately, and help determine the heat transfer and forces from the wall and also flow features as separation.

Near the wall the viscous sub layer has very steeped gradient that the normal mesh would not be enough to capture it, using a prism layers mesher will help capture this gradient, what will give more accurate results.

The prism layers mesher has some properties that are used to control it:

- Number of prism layers.

The user can control the number of prism layers that is generated inside the prism layers by setting a specific number.

- Prism layer total thickness.

The overall thickness for the prism layers can be defined by the user using this property.

- Prism layer stretching.

Prism layer stretching is the ratio between the thickness of each layer and the next layer.

The volume mesher has some requirements that should be fulfilled before the mesher is executed. The surface should be closed, manifold and non-intersecting. For fixing these errors, see Section 3.4.1.

Often the cell quality issues in the volume mesh can be tracked back to the surface mesh face quality, it is recommended that the same setting for the volume mesh should be used for the surface mesh. CD-adapco (2014).

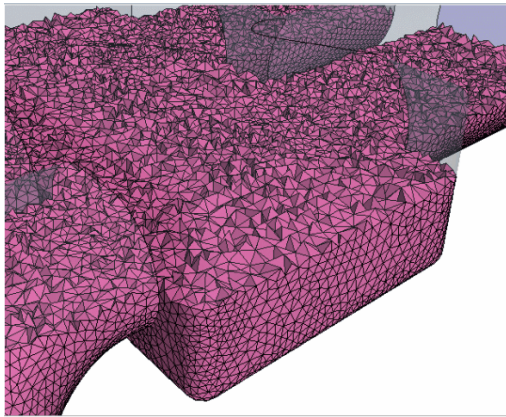


Figure 8 tetrahedral meshes, taken from CD-adapco (2014) manual.

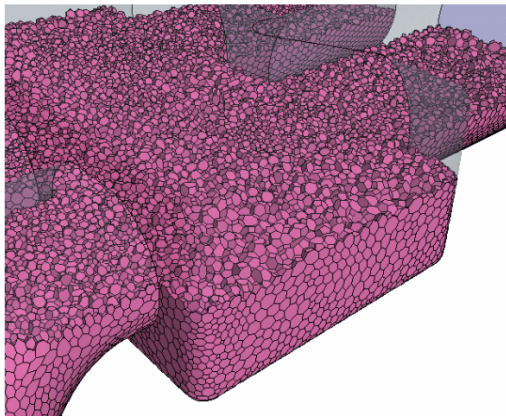


Figure 9 Polyhedral mesh, taken from CD-adapco (2014) manual.

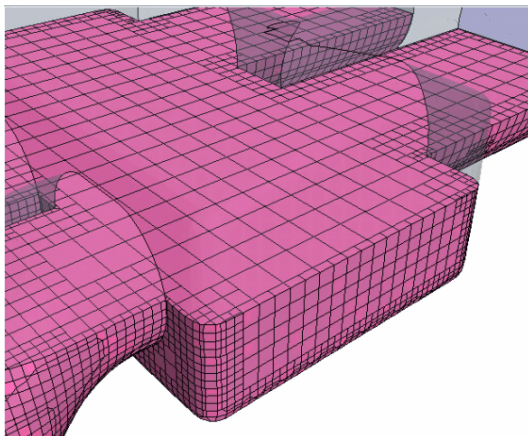


Figure 10 Trimmed mesh, taken from CD-adapco (2014) manual.

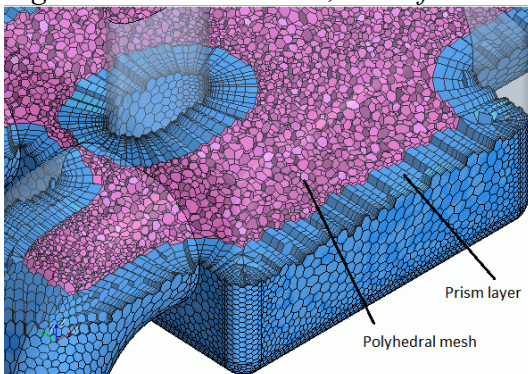


Figure 11 Advancing layer mesher, taken from CD-adapco (2014) manual.

## 2.5 Modeling physics

This section deals with the physics models available in STAR-CMM+, when each model should be selected and what they do.

There are varieties of physics models in STAR-CCM+ one can choose from. When some models are selected other models has to be selected as well. For example when one select fluid model a flow model has to be selected as well.

The physics models in STAR-CCM+ are:

### 2.5.1 Space models

The space model in STAR-CCM+ has four sub-models for the user to choose from them:

- Axisymmetric model.

This model intends to work on two-dimensional axisymmetric meshes. In this type of space model the boundaries edges that lie on the axis should of type axis, and the mesh should be oriented in a way that the axis of rotation is at  $y=0$  in global coordinate space.

- Shell three-dimensional model.

This model is used when the thickness of the geometry is small enough to assume it as a single cell thickness in the normal direction.

- Two dimensional model

This model is designed to work with two-dimensional meshes and the depth is assumed equal to one unit in SI units.

- Three dimensional model

This model is used when three-dimensional mesh is used.

### 2.5.2 Time models

The time models in STAR-CCM+ are:

- Steady model

This model is used when steady state is the target of the simulation. When this model is selected the changes due to the time are not considered in the results of the simulation. In other words only the spatial derivatives are being considered.

- Harmonic balance model

This model is used when the solution repeats it self with known frequency, and is designed to solve periodic unsteady problems.

- Implicit unsteady model

In this time model an implicit solver is used.

- Explicit unsteady model

In this time model an explicit solver is used.

- PISO unsteady model

This model is used for transient states with small time steps. It is only compatible with simulations using K-Epsilon model and no combustion.

### **2.5.3 Modelling materials**

All the fluids and metals can be modeled in STAR-CCM+ as it provides a large group of all the metals and the fluids. Also the user can select a multi-component gas, liquid or solid and can customize the materials properties.

### **2.5.4 Modelling flow and energy**

For simulating the flow and energy in STAR-CCM+ there are two main models the user can select from them:

- Coupled flow and energy model

The coupled flow model solves the energy, momentum and mass equations at the same time. Coupled flow model is suitable for compressible flows, natural convection and flow with large force and energy sources. Moreover it needs more work to be set up than the segregated flow model, requires more memory, but might converge faster if a good mesh is generated for the model.

The number of iterations needed to reach a solution is independent on the mesh size when using the coupled solver.

- Segregated flow and energy model

The segregated model solves the flow equations for each variable separately (pressure and velocity) or in uncoupled way. This model is best for high Mach number cases, incompressible and mildly compressible flows. It has the advantage over the coupled model when the computational power is an issue.

The number of iterations needed to reach a solution depends on the mesh size when using the segregated solver.

### **2.5.5 Modelling the viscous regime**

STAR-CCM+ gives the user the choice to select on of the three models for the viscous regime depending on the application of the simulation.

- Inviscid flow

Inviscid flow is a flow on an ideal fluid, which means that the fluid viscosity is neglected and it will have no effect on the simulation results. The boundary layers are not solved and this causes a significant reduction in the computation power needed for the simulations.

- Laminar flow

This model is used when the flow is at low velocities and there is no disruption in the layers, the fluid flow in parallel layers. It is suitable when the flow has low Reynolds number so that transition to turbulence flow does not occur.

- Turbulent flow

Turbulent flow is characterized by chaotic, instability and irregular motion in space and time. This model is suitable for most of the cases, because turbulence affects most of the flows around us.

STAR-CCM+ has many turbulence models that are used. In this report, only the most common used models are going to be discussed.

1. K- Epsilon model:

A K-Epsilon model is the most common model used in CFD to simulate mean flow characteristics for turbulent flow conditions. The model attempts to predict turbulence by two partial differential equations for two variables. One variable is the kinetic energy  $\kappa$  and the second is the dissipation rate  $\mathcal{E}$ .

2. K-omega model:

This model is a common two-equation turbulence model. That is used as a closure for the Reynolds-averaged Navier–Stokes equations. It also uses two variables to predict turbulence. This model has two equations to be solved, the first for the kinetic energy  $\kappa$  and the second for the specific dissipation rate  $\omega$ .

## 2.5.6 Modelling wall treatment

Wall treatment is a group of assumptions that are used in STAR-CCM+ to model the near wall for each turbulence model. There are three types of wall treatment in STAR-CCM+:

1. High wall treatment:

In the approach it is assumed that the first cell from the wall lies in the logarithmic region of the boundary layer,  $y^+ \geq 30$ . This treatment is suitable for models that do not damp the turbulence in the near wall region.

2. Low wall treatment:

In this treatment it is assumed that the first cell from the wall lies within the viscous sub layer,  $y^+ \leq 1$ . In this model, the viscous sub layer is resolved. This treatment is suitable for the low Reynolds number turbulence models.

3. The all wall treatment:

This is a hybrid approach to enable low wall treatment for fine meshes and high wall treatment for coarse meshes,  $1 < y^+ \leq 30$ . CD-adapco (2014).

### 3 The Experiment

An experiment was carried out to have an idea about how the heater will behave in real life and operation conditions.

The experiment took place in Eldi workshop in Stockholm. The setup for the experiment was as follow, the heater was connected to a tank of 30-liter capacity, the water in the tank has 19° C of temperature, a flow meter was connected to the outlet and thermometer was used to read the temperature of the water in the tank. The Figure below shows the experiment setup. Photos from the experiment are available in the appendix Section (7.1).

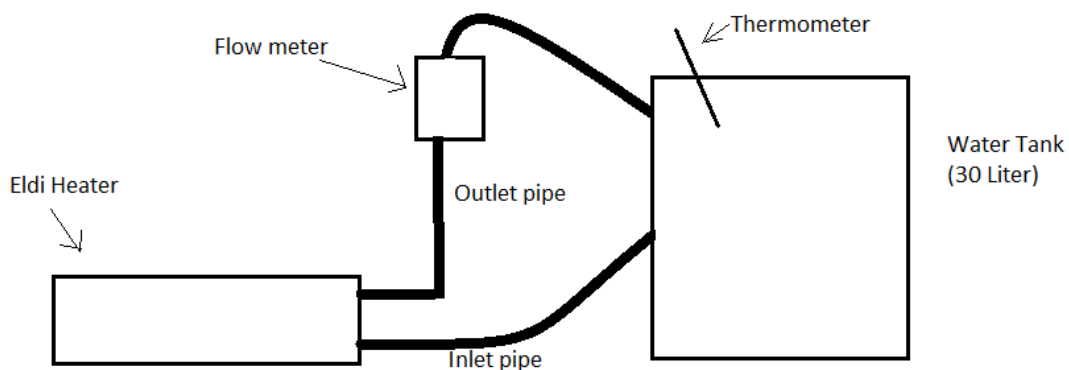


Figure 12 Experiment setup

The starting temperature of the water was 19°C as mentioned before. The pump of the heater was switched on for a few seconds before turning on the heating elements, so the transient state of the flow at the beginning does not affect the temperature measuring. The flow rate and the temperature of the water were registered every minute.

The water is heated until reached a temperature of 70°C then the thermostat switched off the heating elements automatically.

This experiment was carried out for two units each one has a heating source of 9800 W, but only the results for one unit is registered in this report, the other unit was tested only to validate the results. The table below shows the flow-rate and temperature registered each minute.

Table 1 Experiments results for Eldi heater 9800 W

Time [min]	Flow rate [L/min]	Temperature [°C]
0	0	19.0
1	13.5	19.8
2	13.4	24.1
3	13.7	27.6
4	13.6	31.7
5	13.7	35.8
6	13.4	39.7
7	13.6	43.4

8	13.7	47.3
9	13.6	51.2
10	13.5	55.3
11	13.6	58.8
12	13.6	62.6
13	13.8	66.3
14	13.5	70

From the above table one can calculate the average increase in temperature of the water every two minutes. The two minutes interval was selected because it is the time roughly needed for the whole water in the tank to be heated by the heater. By dividing the tank capacity by the flow rate one can calculate the time needed for the water in the tank to be heated providing that the flow-rate is measured.

$$\frac{\text{tank capacity (30 liter)}}{\text{average flow rate (13.6)}} = 2.2 \text{ min} \quad (1)$$

*Table 2 Increase in temperature*

Time [min]	Temperature [°C]	Increase in temperature [°C]
0	19.0	0
2	24.1	5.1
4	31.7	7.6
6	39.7	8.0
8	47.3	7.6
10	55.3	8.0
12	62.6	7.3
14	70	7.4

By calculating the average increase in temperature from the above Table, one can use this average to compare it with the result from the simulation to validate the simulation. The difference between the inlet temperature and the outlet temperature of the water from the simulations should be equal to the average increase from the experiment in ideal world.

The average increase in the temperature from the experiment was found to be 7.2°C.

## 4 Modelling and Results

### 4.1 Geometry

Different geometries are used for the simulations additional to the original one. The idea is to observe how the change in the geometry will affect the efficiency of the heater in terms of the temperature distribution in the outlet. For all the simulations, the boundary conditions are kept constant to focus only on the effect of the geometry. All geometries were prepared by using the repair surface tools provided by STARCCM+ see Section (2.3).

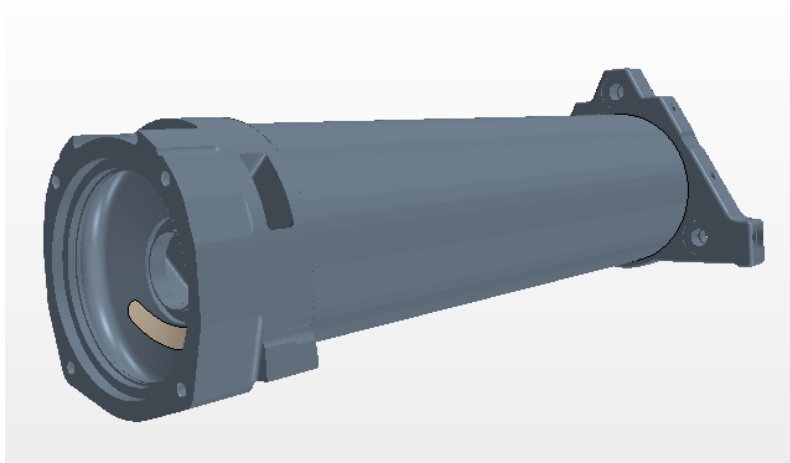


*Figure 13 Original model*

### 4.2 Boundary conditions

The boundary conditions for all the simulations are kept the same. The inlet water has a temperature of  $19^{\circ}\text{C}$ . This temperature is chosen to be consistent with experiment where the inlet temperature is  $19^{\circ}\text{C}$  and the flow rate is  $18\text{ L/min}$ , which is acquired from the data of the pump that is used for the heating element. Nevertheless, when the flow rate is measured it was found to be  $13.6\text{L/min}$ . Hence, it was decided to run the simulation for the original model two times using a flow rate of  $18$  and  $13.6\text{L/min}$  to cover all the possibilities. Regarding the new models the simulation will be run using  $18\text{L/min}$  flow rate and if the results from the simulation show improvement then the same model will be simulated using  $13.6\text{ L/min}$ , this arrangement due to limitation in time and computational power.

The total heat source coming from the elements is  $9800\text{W}$  and the pressure at the outlet is  $0.2\text{ bar}$ . The Figure below shows the boundary conditions for one of the models.

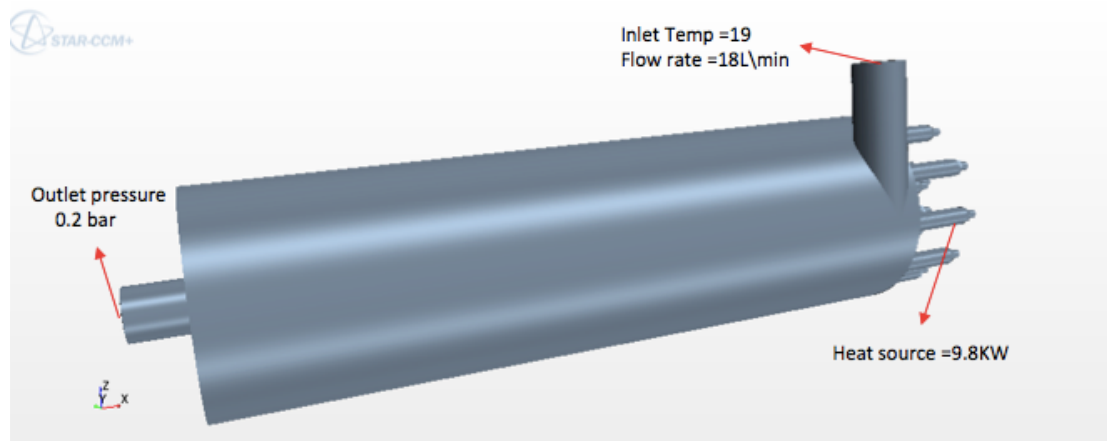


Figure 14 Boundary conditions

### 4.3 Mesh refinement

Mesh refinement study was carried out, because the mesh quality is of great importance for the accuracy of the simulation. A good quality mesh will make the simulation converge faster and the model will have less bad cells.

The base size of the mesh was altered between 0.5, 1,3 and 5 mm to observe the effect on the result for different size mesh. The smaller the mesh base size the larger the number of cells, hence the longer time it takes for the simulation to converge. Therefore, the optimum solution was to find a base size that is not very small and at the same time give accurate results.

The original model was used for the mesh study and to choose which size is the best for the simulations. Due to time limitation the mesh that is assumed the best was used for the other models.

The table below shows the effect of the base size for the mesh on the number of cells. The prism layers are kept only two, because it was found that the prisms layers affect the number of cell greatly. Hence, a separate study on the affect of the prisms layers on the number of cells was conducted.

Table 3 Number of cells based on the base size

Base size	Prism layers	Number of cells
5mm	2	329,819
3mm	2	1,019,928
1mm	2	1,797,506
0.5mm	2	3,132,879

The prism layers affect the accuracy in the region where the fluid meets the metal. In our case, this area has significant importance, because it directly affects the heat transfer from the elements to the fluid. Therefore, a suitable compromise of less number of prism layers and good accuracy should be achieved.

The table below shows the effect of the prism layers number on the cells number.

Table 4 Number of cells based on number of prisms

Base size	Number of prisms	Number of cells
5mm	2	329,819
5mm	4	744,136
5mm	6	905,194
5mm	10	1,227,071

From the table above one can notice the effect of the prisms on the number of cells. Due to computational resource limitation it was found that the maximum number of cells the computer used for the simulations could tolerate is 3 Million cells.

Based on the results from the simulations using different base size mesh, it was found that the 1 mm mesh gives the most accurate results and when used with a combination of 2 prisms layers the number of cells turned out to be 3.1 Million cell, which is within the limit of the computer to run the simulation. The 0.5mm mesh did not add any more details to the result when the results compared to the 1mm mesh results. The Figures below shows the temperature distribution at the outlet for the 1 mm and 0.5mm meshes.

From the below Figures one can see there is no difference in the result, which means using 1 mm mesh will be a smart choice. However, when comparing between the results from the 3mm, 5mm and 1 mm mesh one can notice the rough shapes of the contours that shows the temperature distribution in 3mm and 5mm mesh. This means the results are not accurate enough and the temperature progression is not as smooth as in 1mm and 0.5 mm mesh.

The Figures that show the mesh, residuals and temperature distribution in the water volume for 1mm, 3mm, 5mm and 0.5 mm are available in the appendix Section (7.2).

Finally, the mesh for model 4 has a base size of 2mm instead of 1mm, because the length of the heating elements increased the number of cells to reach 5million, which exceeded the computational power. Hence, the base size for the mesh was increased to 2 mm to reduce the number of cells and without compromising the result accuracy. The confirmation of the 2mm mesh accuracy was done by running a simulation for the original model using mesh with base size of 2mm; the same results were acquired as when running the simulation with 1 mm base size.

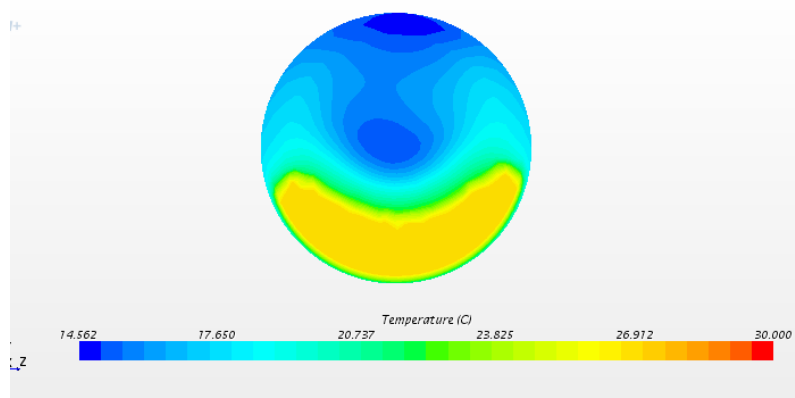


Figure 15 Outlet 1mm base size mesh

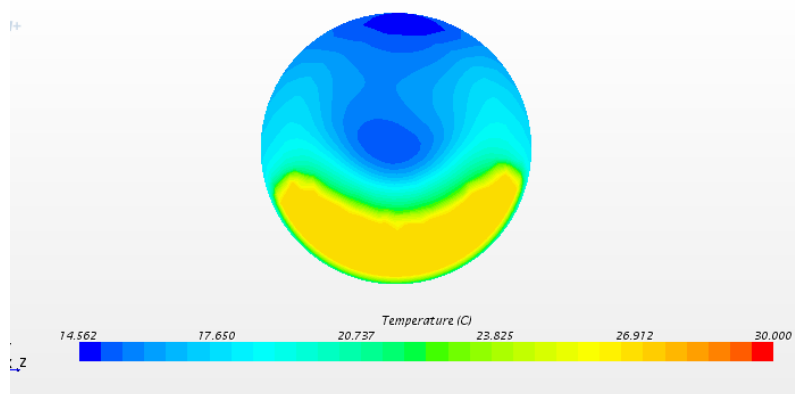


Figure 16 Outlet 0.5 mm base size mesh

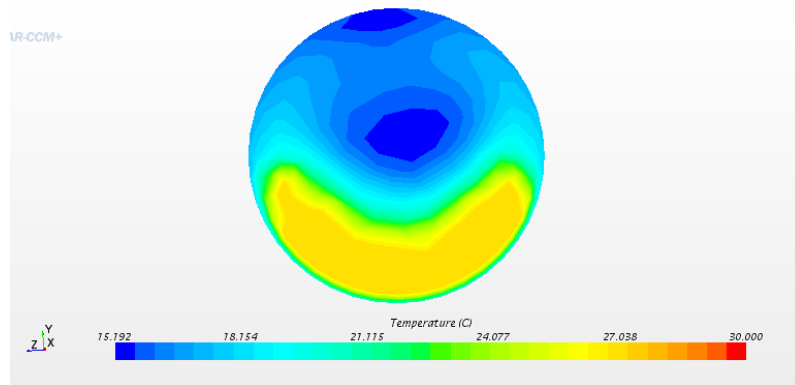


Figure 17 Outlet 3mm base size mesh

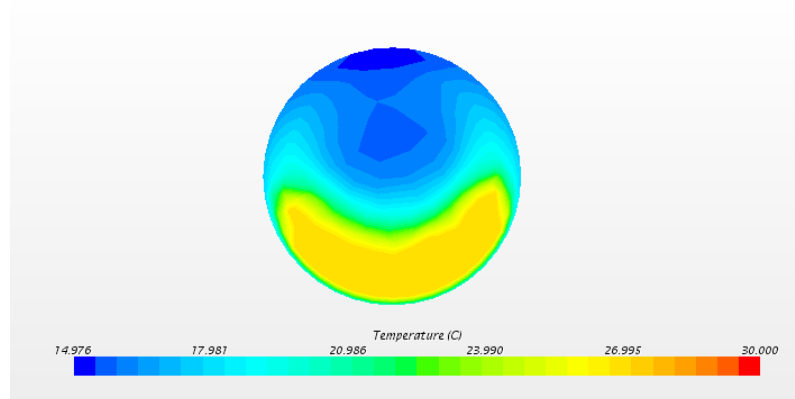


Figure 18 Outlet 5mm base size mesh

## 4.4 Modelling

Modeling the heater in STARCCM+ was done according to the following steps:

### 4.4.1 Building the geometry

The model was built in 3D CAD using Inventor 2015, and then it was imported into STAR CCM+. The surface of the model was prepared for generating the mesh using the tools provided by STAR CCM+. The internal volume of the heater, which should be filled with water, was extracted using a tool in STAR CCM+ called “Extract volume”.

After that, each part in the model was assigned to region, for example assigning the heating elements, thermo-tubes to region steel and the fluid volume to region fluid.

### 4.4.2 Generating the mesh

The models used to generate the mesh were surface remesher, polyhedral mesher and prism layer mesher. The table below shows the settings for generating the mesh.

*Table 5 Mesh continua*

Base size	1mm
Number of prism layers	2
Prism layers stretching	1.5
Prism layers thickness	1.95mm
Surface growth rate	1.3
Relative min size	40% of base size
Relative max size	100% of base size

When the mesh was generated the growth of prism layers were restricted only to the interface of the fluid and the solid region. Because the interface between the fluid and the region is where the heat transfer occurs, hence the prism layer is used to capture this phenomenon.

### 4.4.3 Physics continua

Two physics continua were set up for the solid and fluid region. The model selection for the physics was as follow:

- For the solid region:

*Table 6 Physics models for solid region*

Space	3 dimensional
Time	Steady
Material	Steel
Optional	Segregated solid energy

- For water region:

Table 7 Physics models for water region

Space	3 dimensional
Time	Steady
Material	Water
Flow	Segregated flow
Equation of state	Constant density
Viscous regime	Turbulent
Reynolds-Averaged Turbulence	K-Epsilon Turbulence
Wall treatment	Segregate fluid temperature
Optional	Two layer all $y^+$ treatment

#### 4.4.4 Residuals and mass imbalance

The residuals plot is generated automatically by STAR CCM+ to show the error of the simulation and to show when the simulation is converged. A second plot was generated to examine the accuracy of the simulation is the mass imbalance.

The mass imbalance plot was generated using the following equation:

$$(\text{Total mass flow} \div \text{inlet mass flow}) \times 10 \quad (2)$$

The smaller the number results from the equation the more accurate results achieved.

Finally, a plane sections were created to plot the variables under study, and several scenes were created to visualize the results. The plots for the residuals and mass imbalance can be seen in the appendix Section (7.3).

## 4.5 Results

Each model results will be discussed separately and in the discussion and conclusion a comparison between the models will be discussed.

### 4.5.1 The original model

This model represents the heating unit that is used now by Vehtec to heat the passenger's compartment in the vehicles. The figure below shows the geometry of the original Eldi heater. One can notice that the inlet has an oval shape for this unit and the outlet is circular. The simulation of this model was run twice to simulate the two flow rates 18 and 13.6L/min.

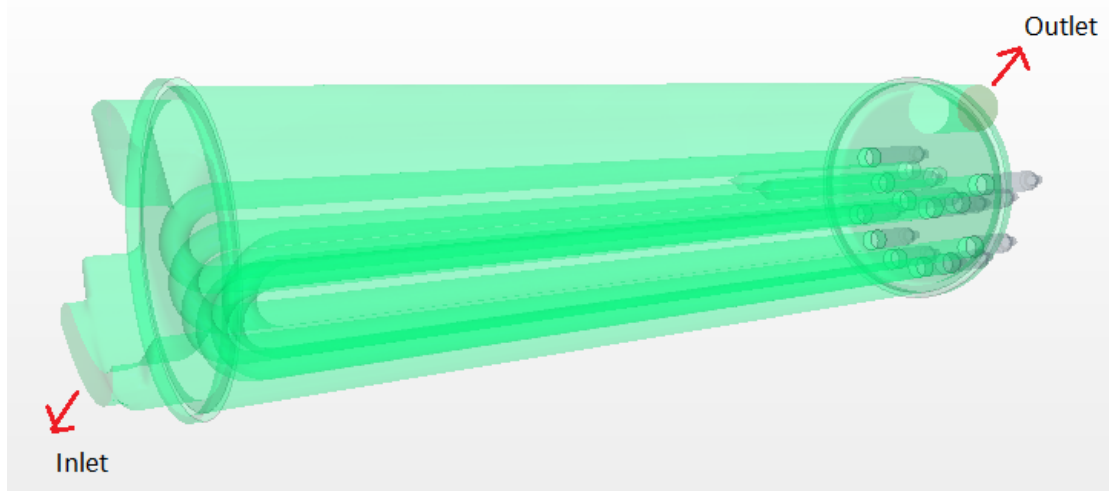


Figure 19 Original model geometry

After running the simulations until it converged the following results were collected:

#### 4.5.1.1 Temperature distribution on the elements

From Figures 20 and 21, one can observe that the heating elements are hotter on the up side than the down side. This means the volume of the water passes through the down side is larger than that passes through the up side, which means the distribution of the water inside the heating unit is not uniform.

#### 4.5.1.2 Streamlines

From Figure 22, one can see that the majority of the flow passes through the down side of the elements and goes through the outlet. Moreover, the water on the topside keeps circulating inside the heater for a longer time what makes it hotter than the water in the bottom side. Unfortunately, only a small amount of this water in the upside leaves the unit, on the other side the majority of the water that leaves the heater is from the bottom side. The water from the bottom side is not as hot as the one from the upside, because it leaves the heater faster. The streamlines for both flow rates 18 and 13.6l/min are similar, hence there was no need to show the streamlines for 13.6l/min simulation.

#### 4.5.1.3 Temperature distribution over the water volume

The Figures 23 and 24 represent the water volume inside the heating unit. This figure validates the previous assumption that the water in the topside is warmer than the bottom side.

#### 4.5.1.4 Outlet temperature

Figures 25 and 26 show the temperature distribution on the outlet surface, the average temperature for the surfaces is 26.5°C for 18l/min flow rate and 28.7°C for the 13.6l/min flow rate.

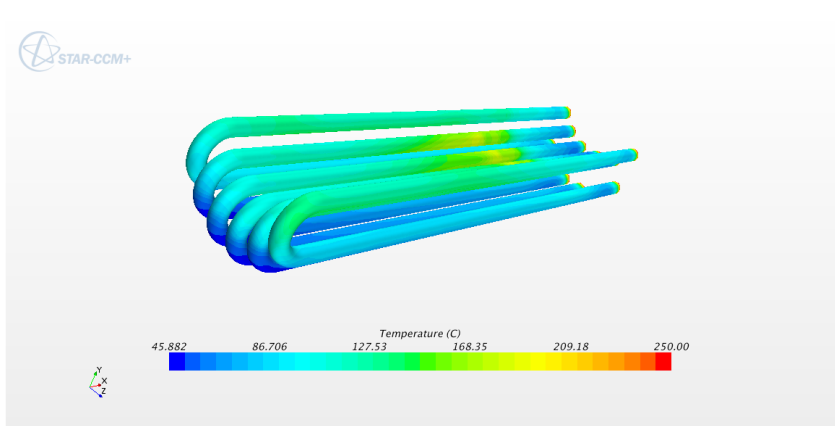


Figure 20 Heating elements of original model, 18l/min flow rate

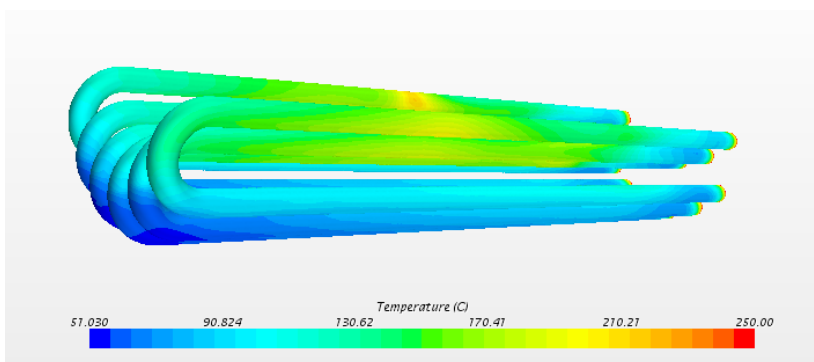


Figure 21 Heating elements of original model, 13.6l/min flow rate

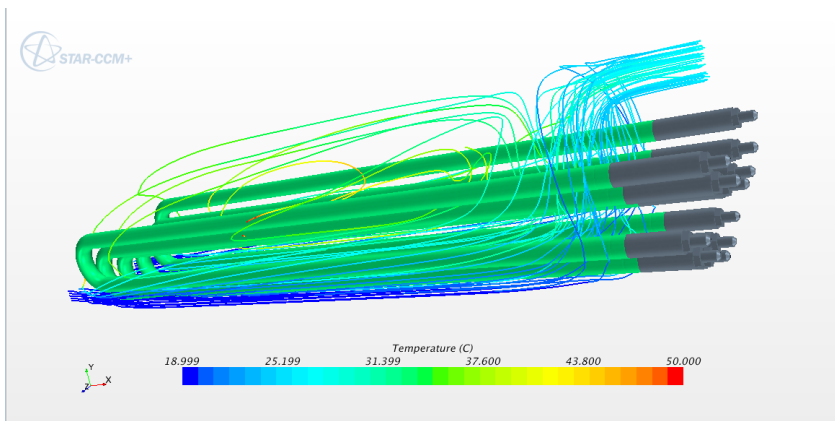


Figure 22 Streamlines of original model, 18l/min flow rate

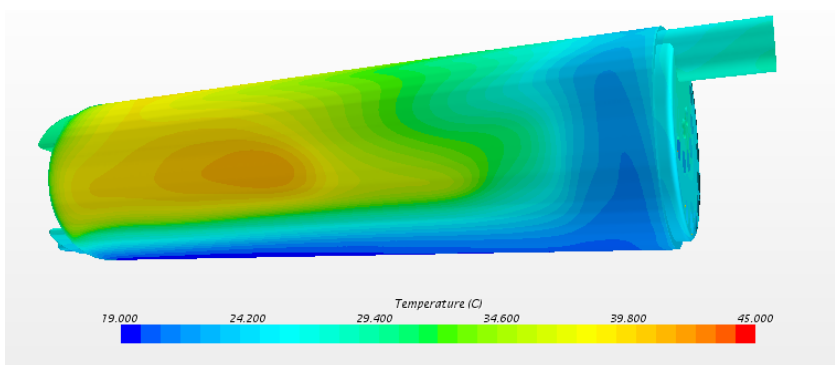


Figure 23 Water volume, 13.6l/min flow rate

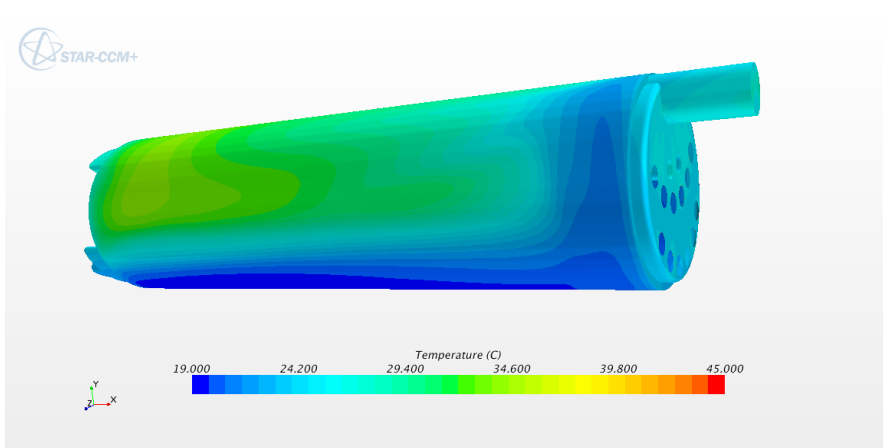


Figure 24 Water volume, 18l/min flow rate

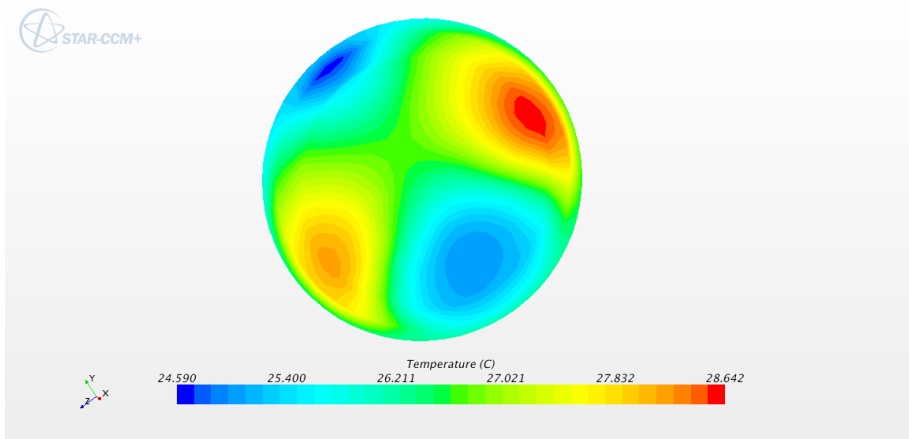


Figure 25 Outlet temperature of original model 18l/min flow rate

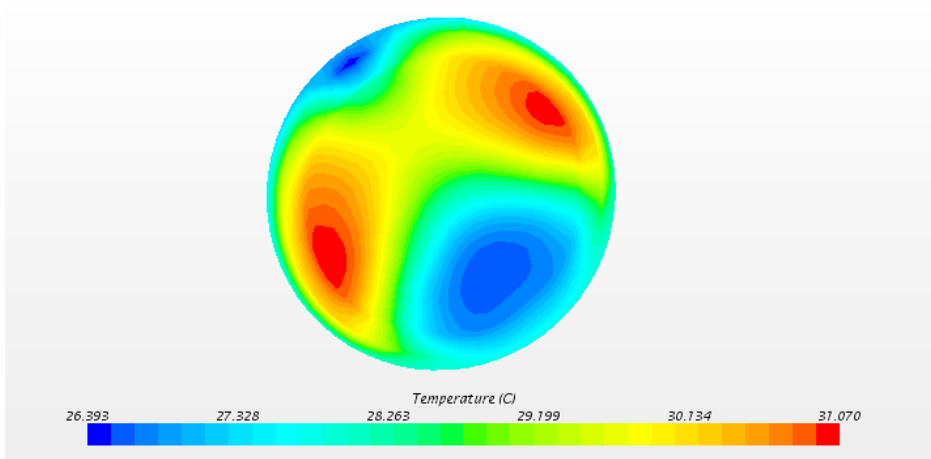


Figure 26 Outlet temperature 13.6l/min flow rate

## 4.5.2 Model 1

This model is the first attempt to improve the efficiency of the heating unit. The idea behind the design of this model is to create turbulence inside the heating unit, which will increase the heat transfer between the water and the heating elements. The inlet is situated on the side of the heating unit, therefore the water will move in spiral shape when it enters the heating unit. Moreover, the heating elements were distributed inside the volume in a uniformed way that it thought to give better heat transfer between the heating elements and the water. The simulation for this model was carried out using a flow rate of 18l/min.

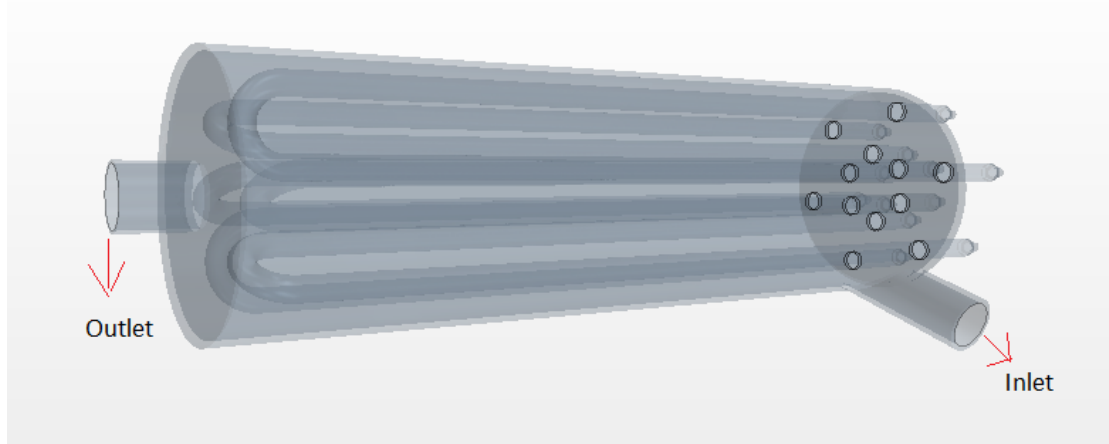


Figure 27 Model 1 geometry

### 4.5.2.1 Temperature distribution on the elements

One can see from Figure 28 that the element temperature in the middle is higher than the edges and the coolest part is the one close to the inlet.

### 4.5.2.2 Streamlines

From Figure 29, one can notice that the radial motion of the water is the reason behind the lower temperature on the elements part that is closer to the cylinder wall. Meanwhile the water volume in the middle of the cylinder has less motion relatively, which reduce the heat transfer between the water and the elements.

### 4.5.2.3 Temperature distribution over the water volume

Figure 30 shows the gradual heating of the water as it moves through the heating unit, also shows gradual distribution of the temperature, which is opposite to Figure 27 of the original model.

### 4.5.2.4 Outlet temperature

Figure 31 shows the temperature distribution over the outlet surface, the average temperature is 26.5°C.

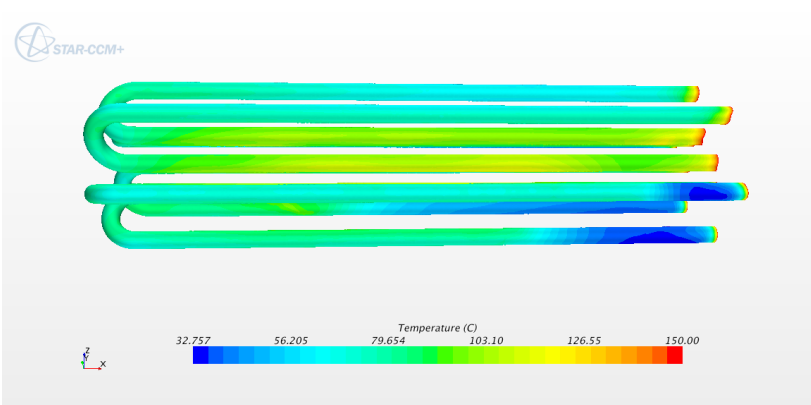


Figure 28 Heating elements of model 1

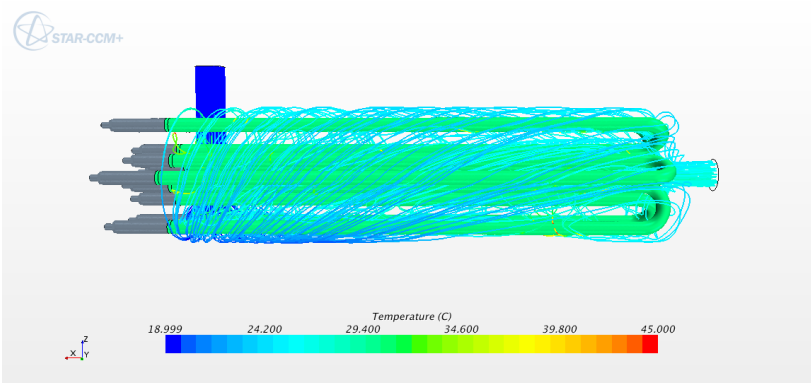


Figure 29 Streamlines of model 1

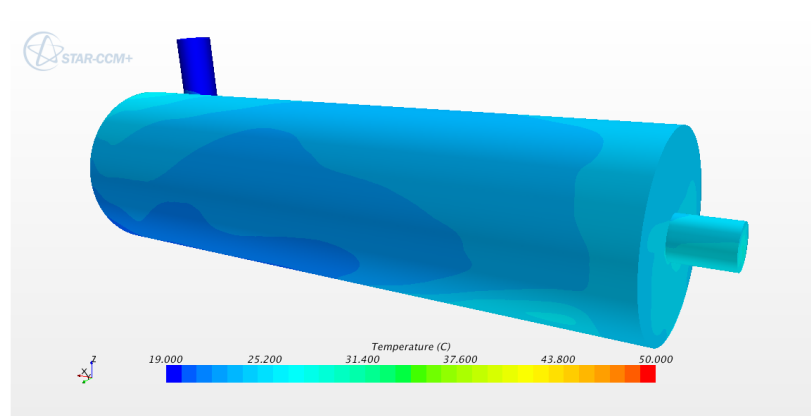


Figure 30 Water volume model 1

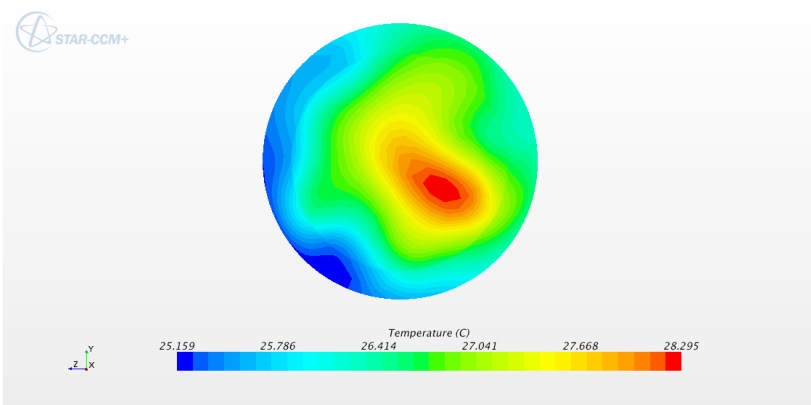


Figure 31 Outlet temperature

### 4.5.3 Model 2

Model 2 is designed with flanges inside to work as obstacles for the water flow, hence the water will stay in contact with the heating elements for longer period and the turbulence should increase. As a result, the heat transfer to the water is expected to increase. This model is simulated using 18 and 13.6 l/min flow rates. The Figures from the 13.6 l/min flow rate simulation can be seen in the appendix Section (7.3).

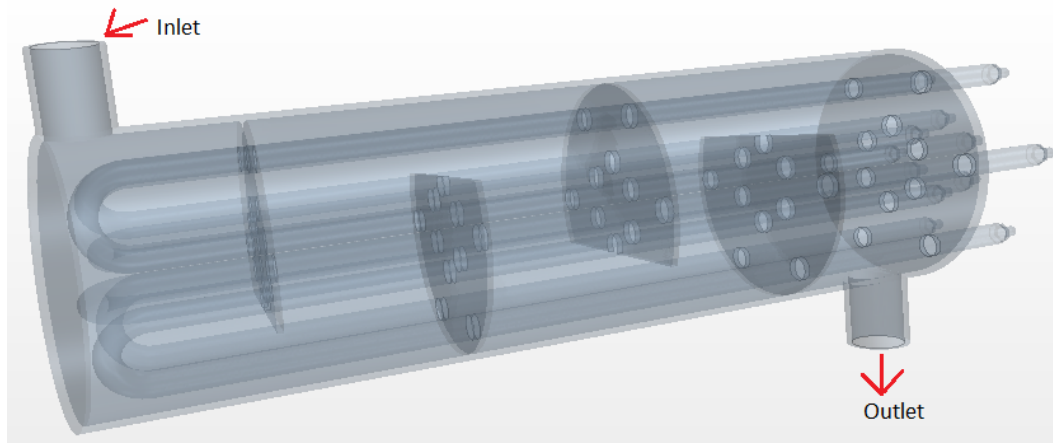


Figure 32 Model 2 geometry

#### 4.5.3.1 Streamlines

Figure 33 present the streamlines generated for the simulation of model 2. The flanges deflects the water, hence it should increase the turbulence and the heat transfer rate.

#### 4.5.3.2 Temperature distribution over the heating elements

One can see from Figure 34 that the temperature distribution on the heating elements is not uniform.

#### 4.5.3.3 Water volume

From Figure 35, one can see the gradual heating of the water as it passes through the heating unit.

#### 4.5.3.4 Outlet temperature

Figure 36 shows the temperature distribution over the outlet, the average surface temperature is 26.8°C for 18l/min flow rate simulation and 29.3°C for 13.6l/min flow rate. The Figures of the second simulation with 13.6l/min flow rate are in Section (7.3).

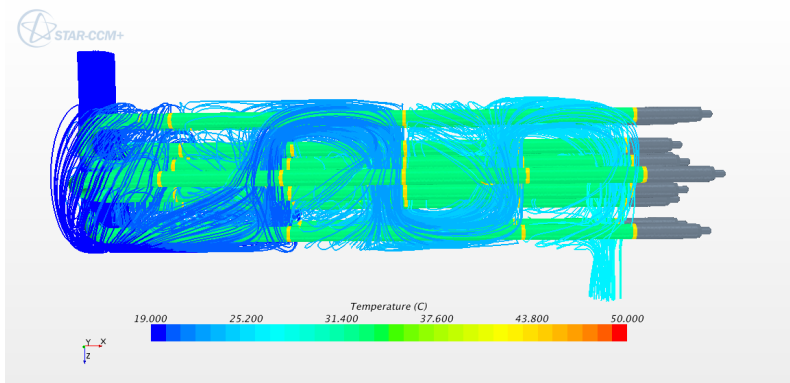


Figure 33 Streamlines of model 2, 18L/min flow rate

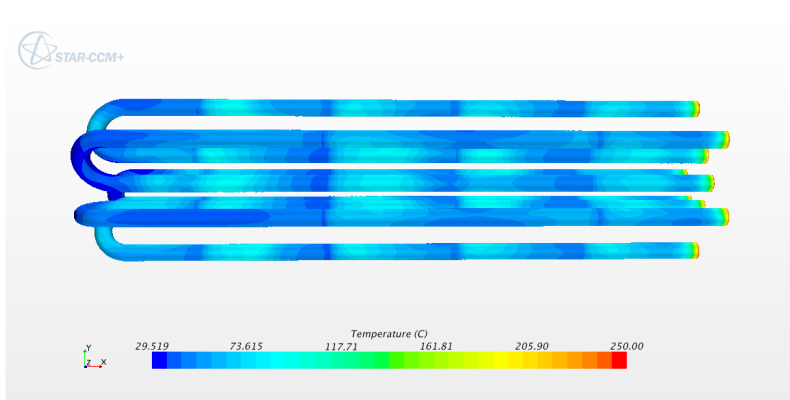


Figure 34 Heating elements of model 2, 18L/min flow rate

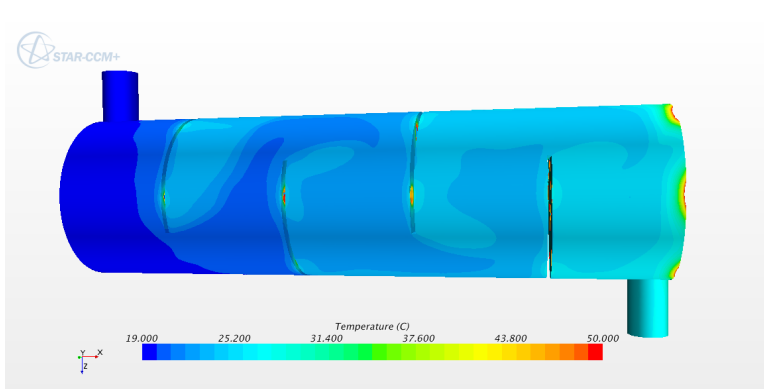


Figure 35 Water volume of model 2, 18L/min flow rate

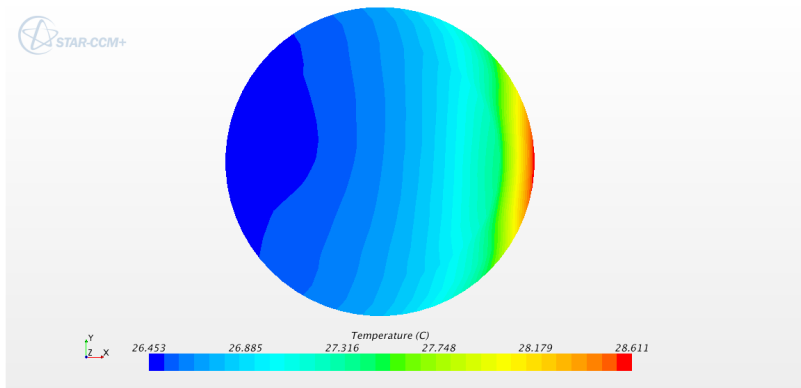


Figure 36 Outlet temperature of model 2, 18L/min flow rate

#### 4.5.4 Model 3

The purpose from this model was to observe the effect of increasing the surface area on the heat transfer from the elements to the water. It is known from the physics that the transfer of heat increases when the surface area increase. The number of heating elements in this model is doubled comparing to the previous models.

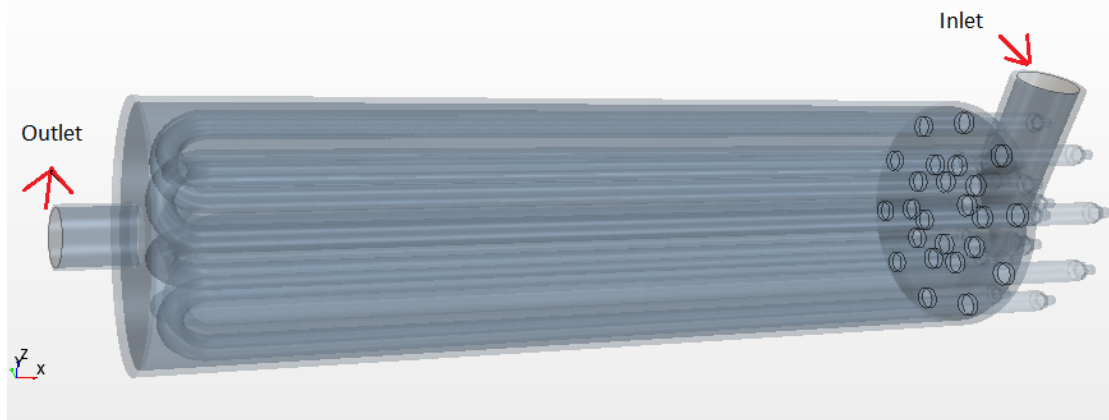


Figure 37 Model 3 geometry

##### 4.5.4.1 Streamlines

The Figure 38 shows the streamlines of model 3 and how the water moves inside the heating unit.

##### 4.5.4.2 Heating elements temperature

One can see from Figure 39 that the part of the heating elements near to inlet is the coldest and the middle part of the heating elements is the hottest.

##### 4.5.4.3 Water volume

Figure 40 shows the temperature distribution on the water volume of model 3.

##### 4.5.4.4 Outlet temperature

Figure 41 represents the temperature distribution on the outlet with average of 26.4°C.

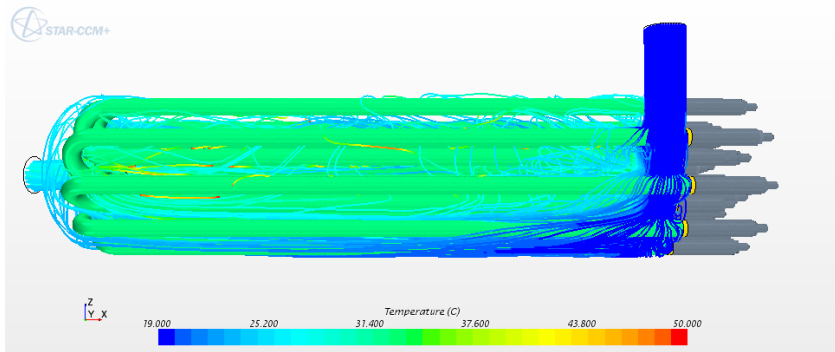


Figure 38 Streamlines of model 3

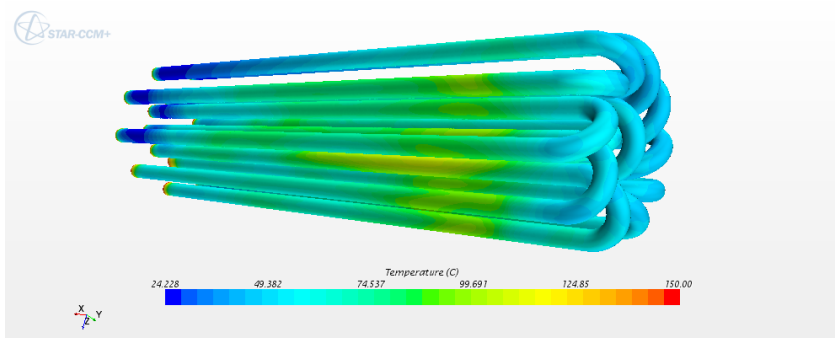


Figure 39 Heating elements temperature of model 3

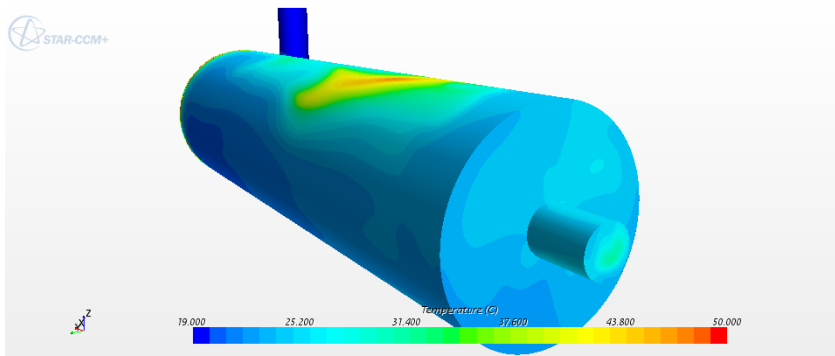


Figure 40 Water volume of model 3

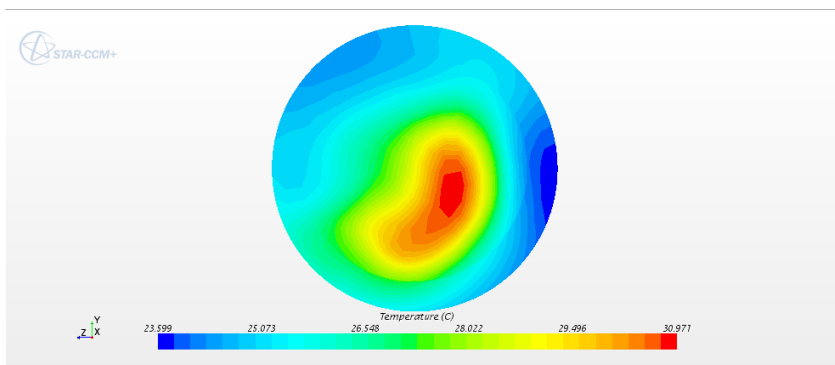


Figure 41 Outlet temperature

### 4.5.5 Model 4

Model 4 is designed in a way that is thought to be the optimum, by considering the advantages and disadvantages of the previous models. Two flow rates are used to simulate this model, 13.6 and 18 l/min.

The heating elements for this model is designed in spiral shape to increase the surface area without needing to increase the volume of the heating unit.

The Figures resulted for the simulation with flow rate 13.6 l/min can be found in the appendix Section (7.3).

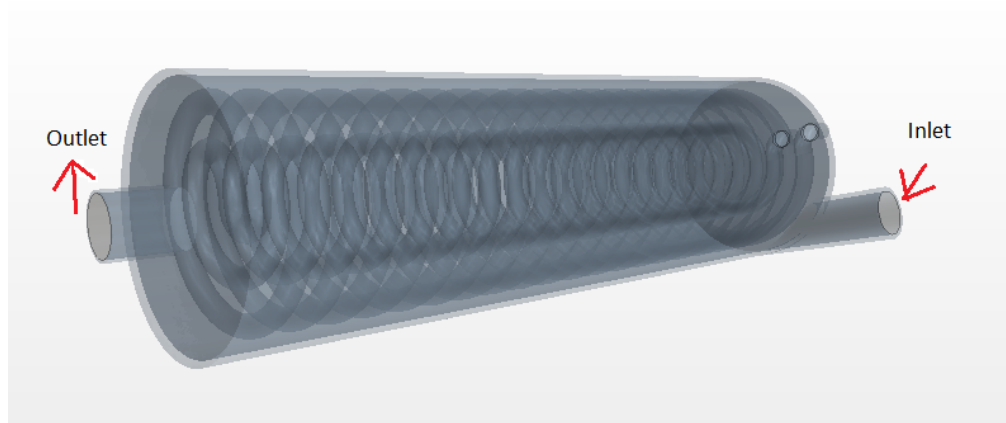


Figure 42 Model 4 geometry

#### 4.5.5.1 Streamlines

Figure 43 shows the streamlines of model 4 when simulated with 18l/min flow rate. The streamlines for 13.6l/min flow rate is not different from Figure 46 only in the temperature of the water, one can see it in the appendix Section (8.3).

#### 4.5.5.2 Heating elements

Figure 44 shows the temperature distribution over the heating elements of model 4. It can be noticed that the inner coil is warmer than the outer coil, which indicate less heat is transferred from the inner coil to the water.

#### 4.5.5.3 Water volume

Figure 45 shows the temperature distribution on the water volume of model 4. The water moves in spiral shape due to the design of the inlet and the heating elements.

#### 4.5.5.4 Outlet temperature

Figure 46 shows the temperature of the water on the outlet, the average temperature is 26.6°C for 18l/min flow rate and for the 13.6l/min flow rate is found to be 29°C. The Figures for the simulation of 13.6l/min can be seen in the appendix Section (7.3).

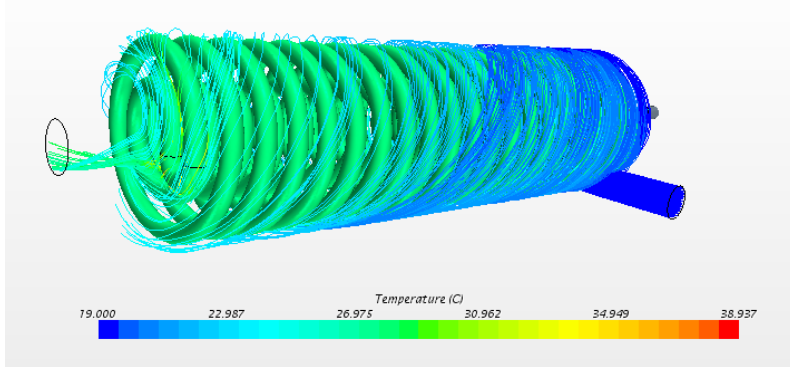


Figure 43 Streamlines, 18l/min flow rate

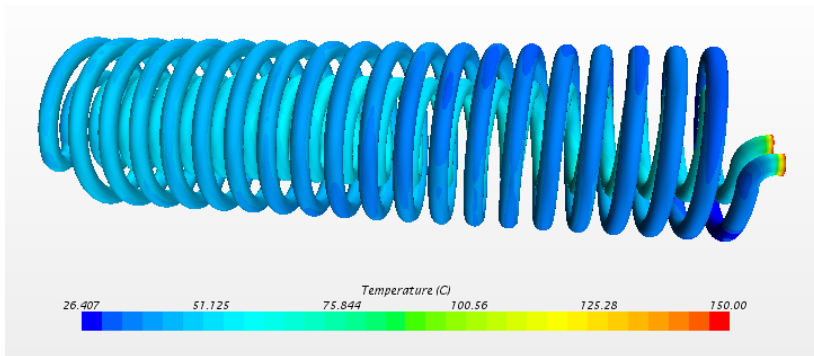


Figure 44 Heating elements, 18l/min flow rate

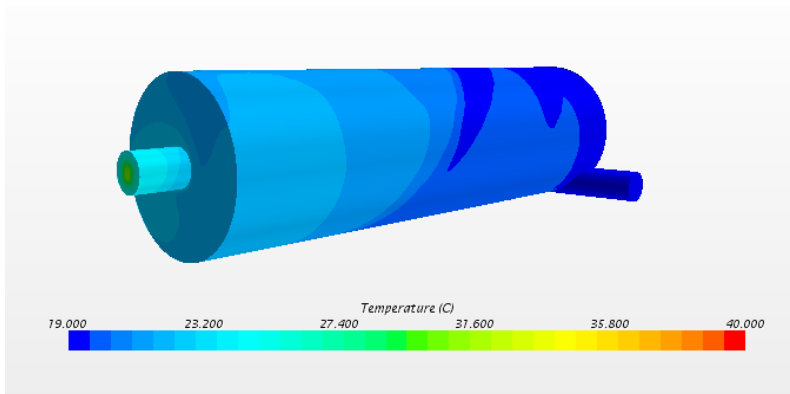


Figure 45 Water volume, 18l/min flow rate

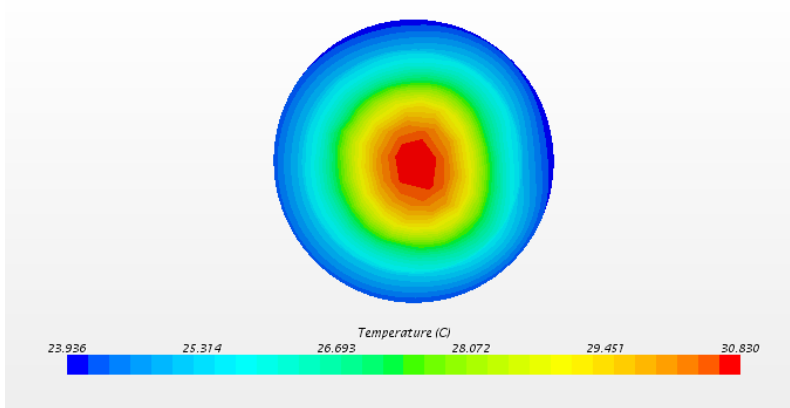


Figure 46 Outlet temperature of model 4, 18l/min flow rate

## 5 Discussion and conclusion

In this chapter the results of the simulations will be discussed:

- Original model:

From looking at the results of the original model, one can notice that the shape of the inlet and the positions of both of the inlet and the outlet cause the water to leave the heater very quickly. Hence, it does not warm to a higher temperature.

Moreover, due to the positions of the inlet, outlet and heating elements a circulation bubble is created in the topside of the heater, which restricts the flow of the water. Therefore, by changing the position of the inlet, outlet and the heating elements one can improve the efficiency of the heating unit.

- Model 1

In this model the inlet shape and position has been altered to check if this could increase the efficiency of the heating unit. Moreover, the heating elements are distributed evenly inside the heating unit. However, instead of all these changes the outlet temperature remained the same as the original model.

- Model 2

From looking at the results of model 2, one can see the flanges succeeded in working as an obstacle for the flow and created more turbulence, which should increase the heat transfer rate from the heating elements to the water.

This model gave the best results as the temperature increased by  $0.3^{\circ}\text{C}$  when the flow rate is 18l/min and  $1^{\circ}\text{C}$  when the flow rate is 13.6l/min.

- Model 3

From looking at the results of model 3, one can see that the streamlines are not similar to the ones from model 1, despite the both models have the same positions of the inlet and the outlet. This non-similarity is probably due to increasing the number of the heating elements, which affect the flow shape.

- Model 4

From looking at the streamlines of model 4, it was observed that the majority of the flow is exposed to the outer coil, which makes the outer coil colder than the inner one due to the heat transfer to the water.

In conclusion, the models that show improvement are model 2 and model 4. Model 2 shows the best result with a temperature increase by 7% and if this increase is reflected on the time needed for the water to be heated to  $70^{\circ}\text{C}$ , then the reduction in time will be 2 minutes, which is 14%.

More simulations are needed in the future to investigate more arrangements for the inlet and outlet positions, plus the heating element shape and surface area.

## 6 References

Versteeg, H.K., Malalasekera, W. (2007): An introduction to computational fluid dynamics: the finite volume method, 2nd edition, Pearson Prentice Hall, Harlow.

CD-adapco (2014): User guide, STAR-CCM+, Version 9.06.

CD-adapco (2012), STAR south east Asian conference, Heat transfer best practice.  
URL: [http://www.cd-adapco.com/sites/default/files/Presentation/Heat-Transfer-Best-Practices-Nov2012\\_PE.pdf](http://www.cd-adapco.com/sites/default/files/Presentation/Heat-Transfer-Best-Practices-Nov2012_PE.pdf)

CD-adapco (2012), STAR south east Asian conference, best practices volume meshing.  
URL: [http://www.cdadapco.com/sites/default/files/Presentation/SEA%20Conference%202012\\_CDadapco\\_VolumeMeshing\\_Used\\_KM.pdf](http://www.cdadapco.com/sites/default/files/Presentation/SEA%20Conference%202012_CDadapco_VolumeMeshing_Used_KM.pdf)

Tel Toro, A. (2012) computational fluid dynamics analysis of butterfly valve performance factors {master thesis}, Utah state university, {Logan, Utah} 2012.

## 7 Appendix

### 7.1 Photos from the experiment

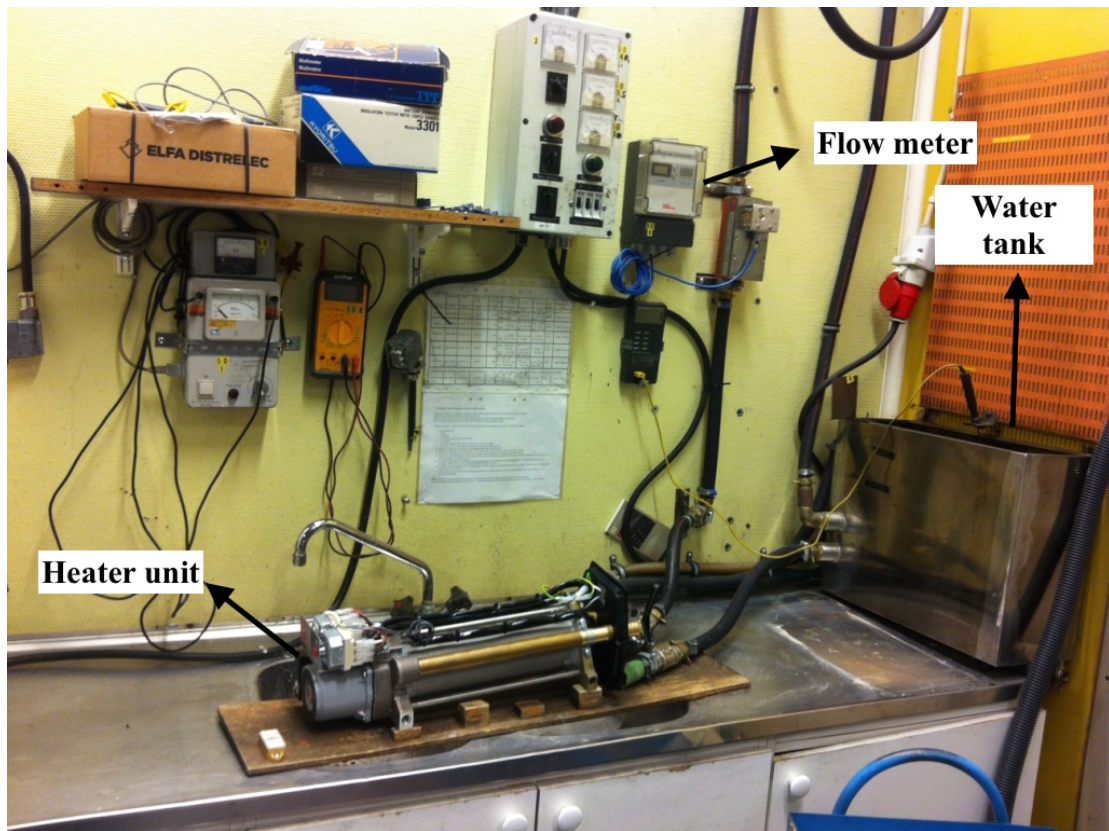


Figure 47 Setup of the experiment

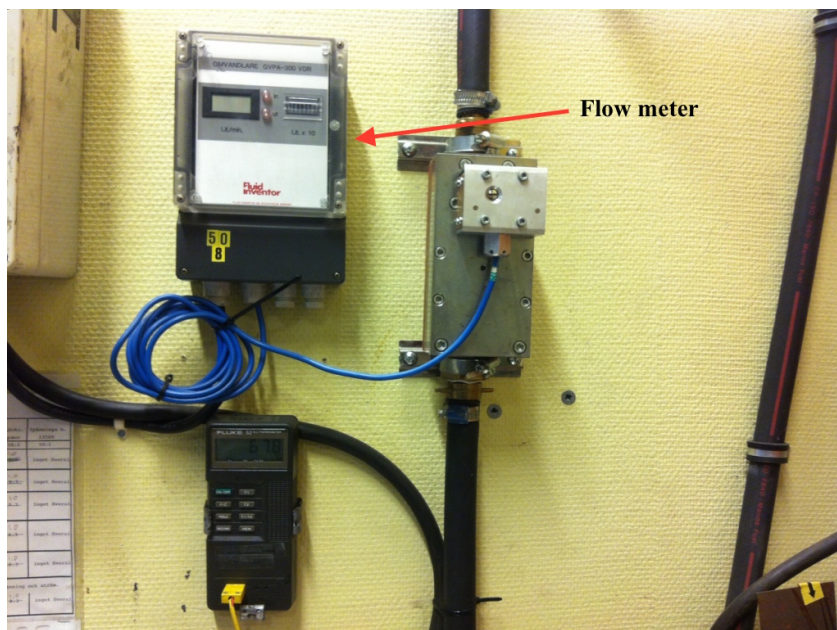


Figure 48 Flow meter

## 7.2 Mesh refinement study



Figure 49 Plane section of 0.5 mm base size mesh

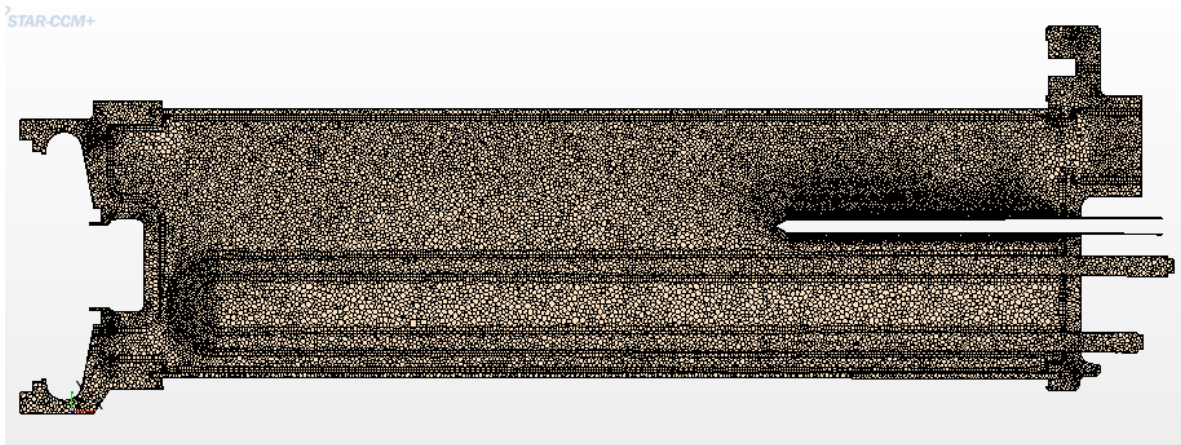


Figure 50 Plane section of 1mm base size mesh



Figure 51 Plane section of 3mm base size mesh

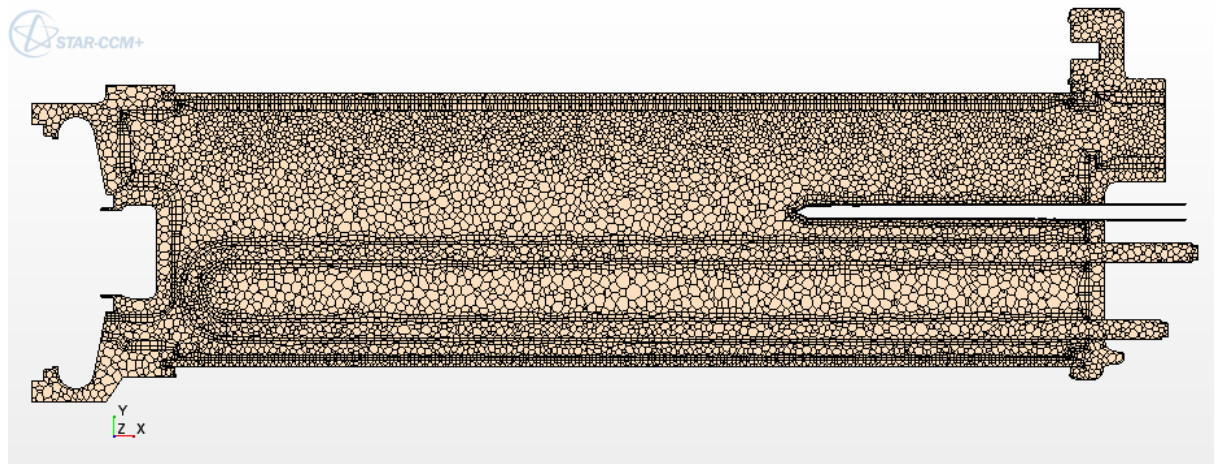


Figure 52 Plane section of 5 mm base size mesh

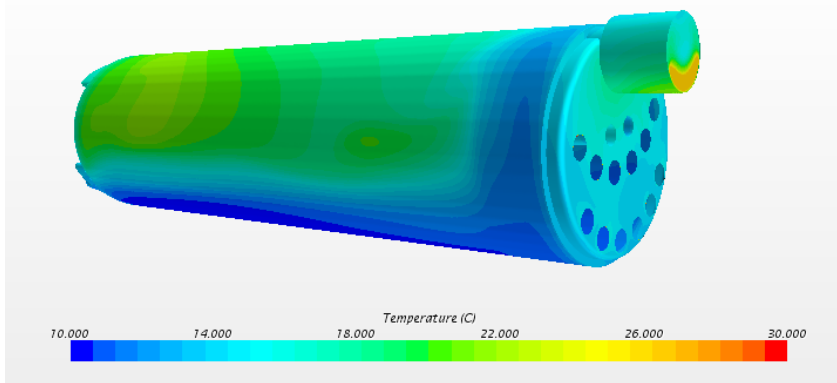


Figure 53 Temperature of water volume, 0.5mm base size mesh

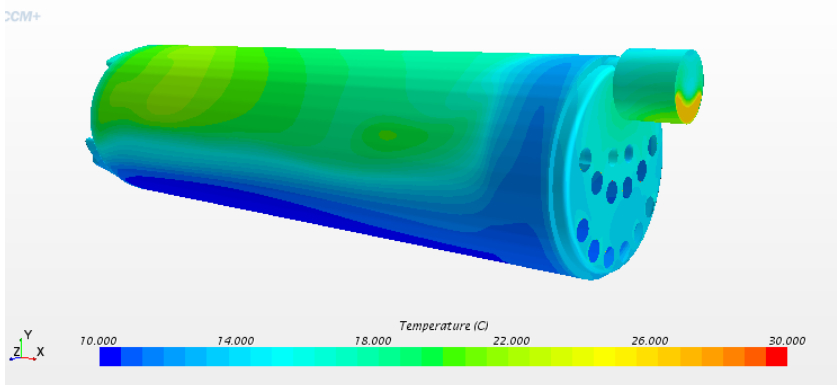


Figure 54 Temperature of water volume, 1mm base size mesh

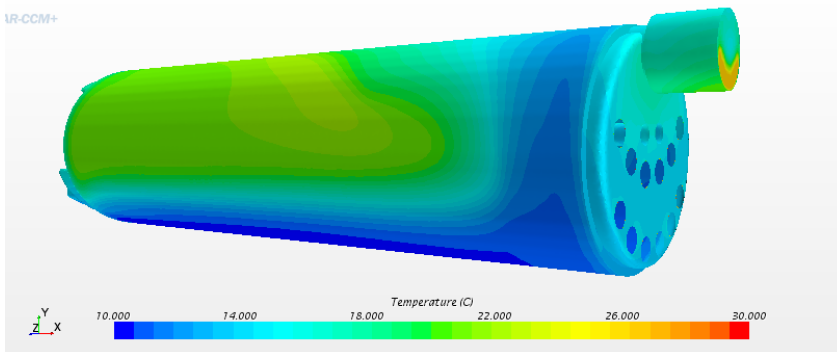


Figure 55 Temperature of water volume, 3mm base size mesh

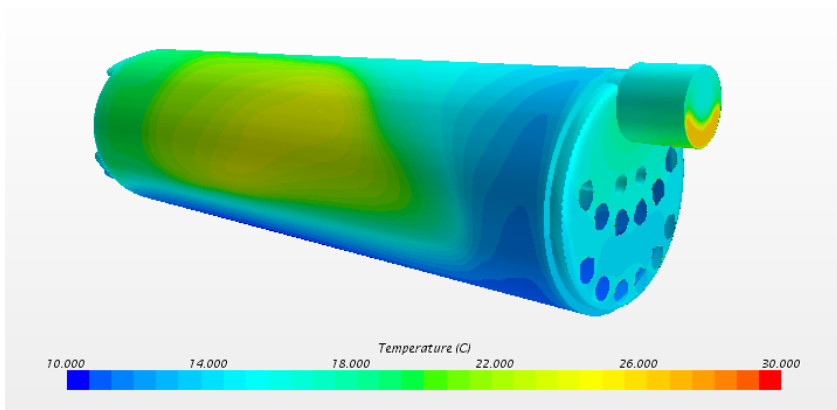


Figure 56 Temperature of water volume, 5mm base size mesh

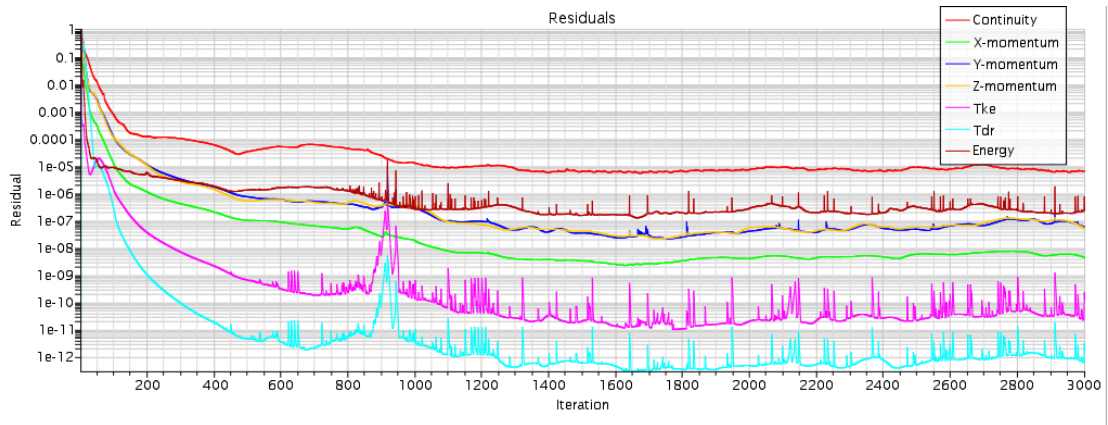


Figure 57 Residuals, 0.5mm base size mesh

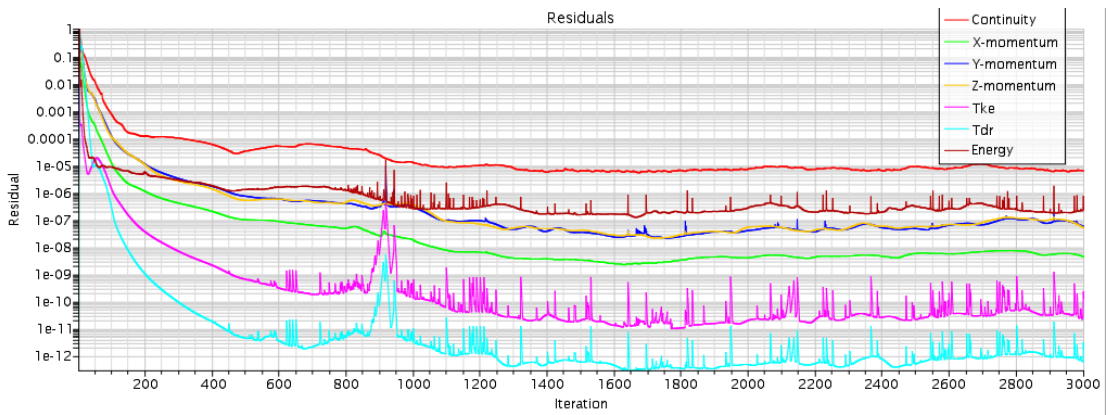


Figure 58 Residuals, 1mm base size mesh

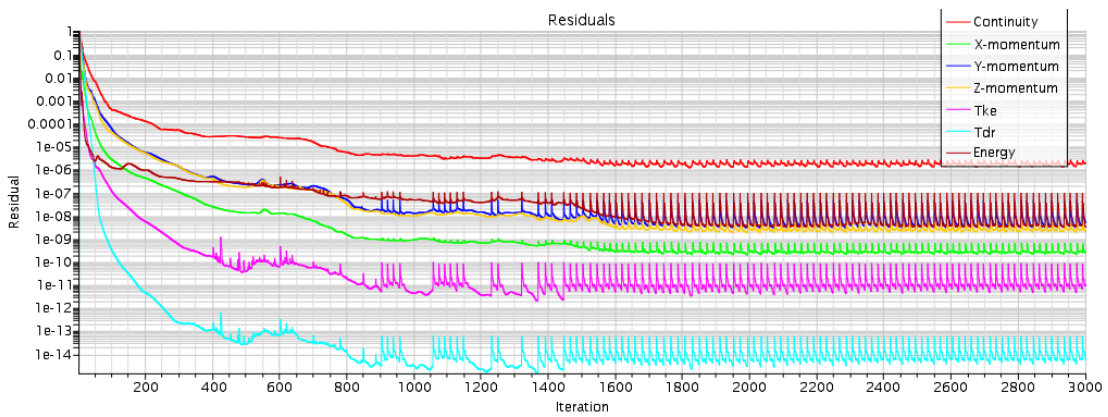


Figure 59 Residuals, 3mm base size mesh

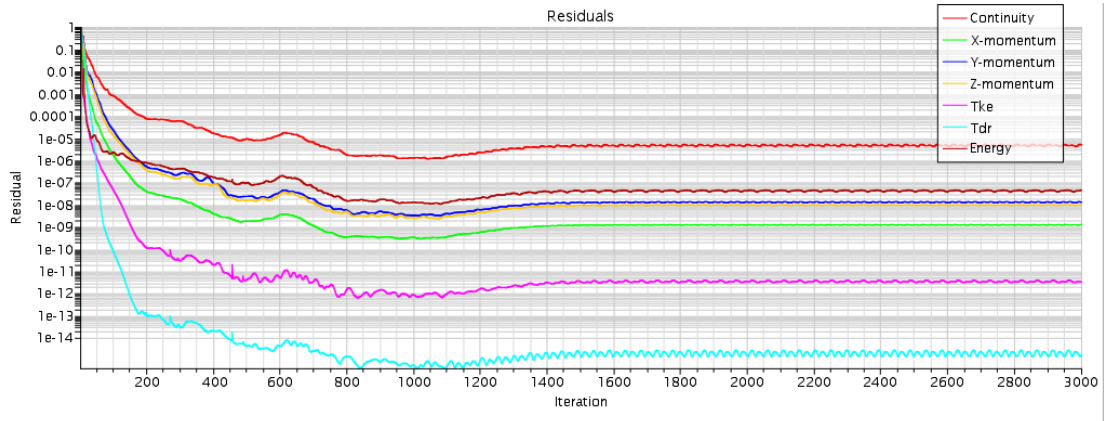


Figure 60 Residuals, 5mm base size mesh

### 7.3 Simulations results

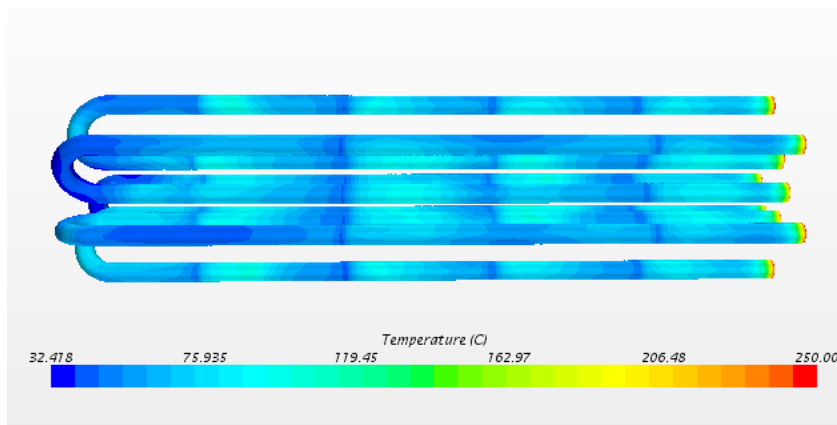


Figure 61 Heating elements of model 2, 13.6l/min flow rate

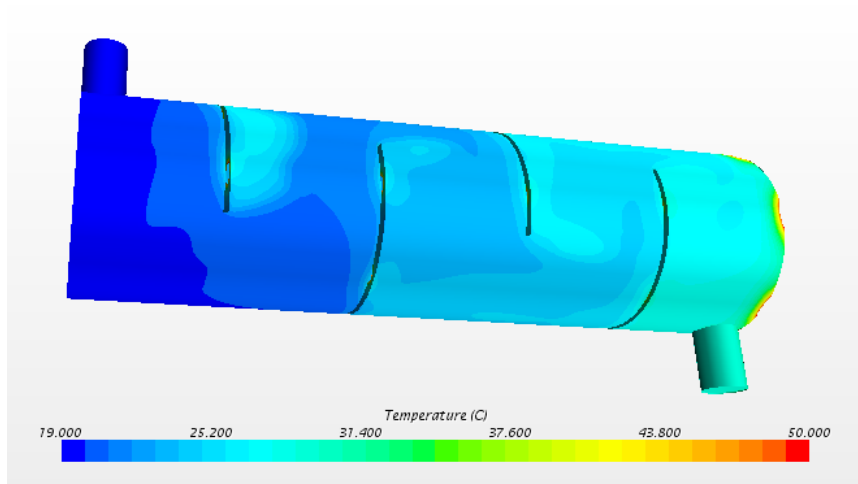


Figure 62 Water volume of model 2, 13.6l/min flow rate

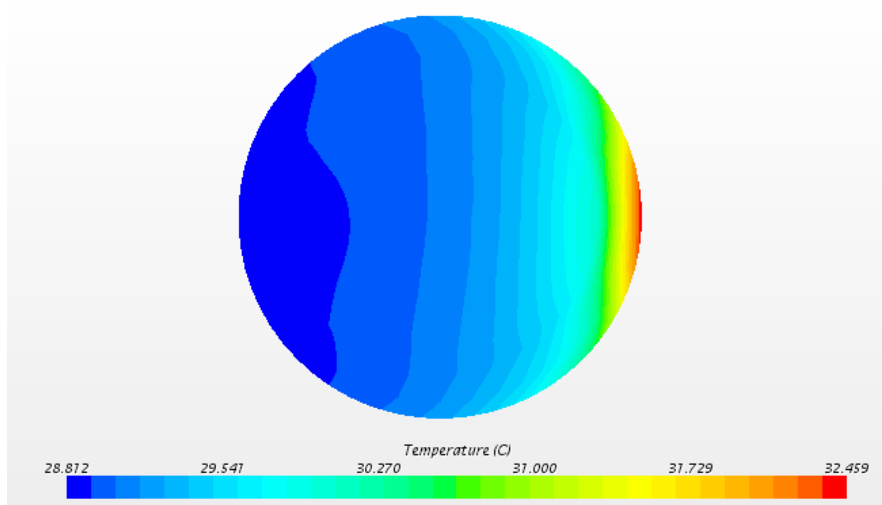


Figure 63 Outlet of model 2, 13.6l/min flow rate

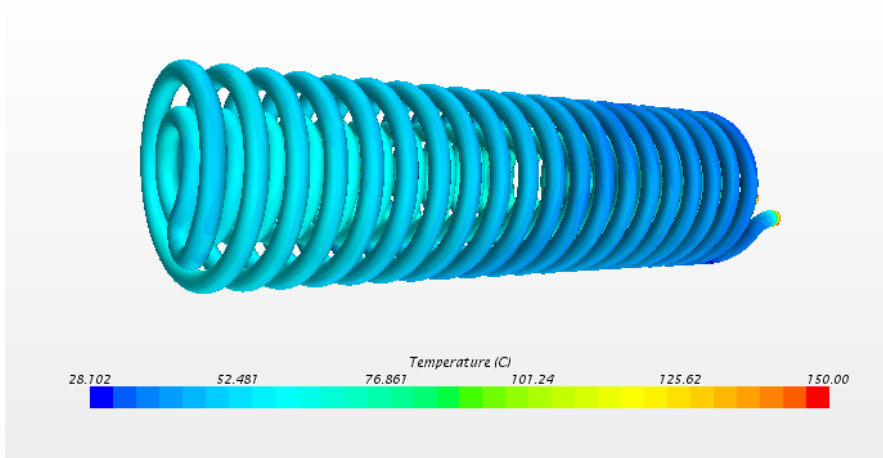


Figure 64 Heating elements of model 4, 13.6l/min flow rate

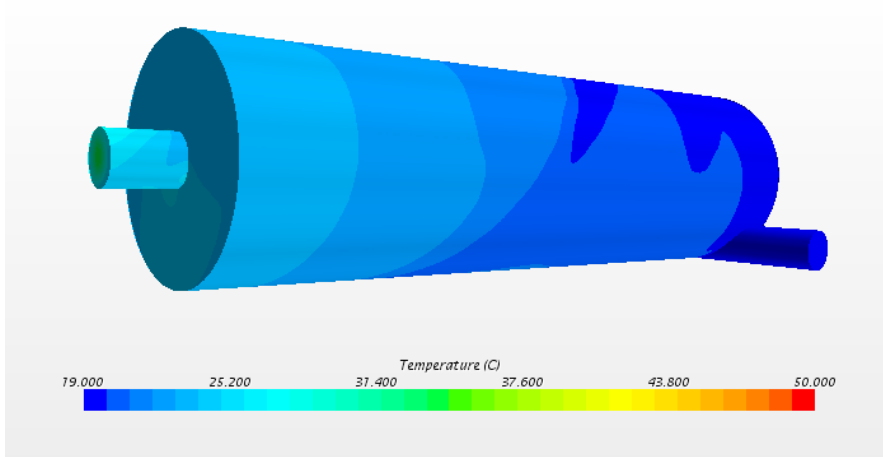


Figure 65 Water volume of model 4, 13.6l/min flow rate

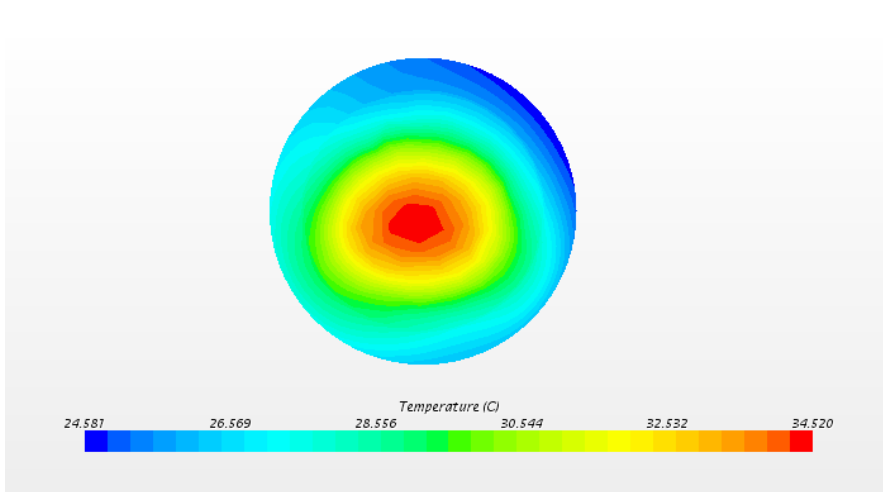


Figure 66 Outlet of model 4, 13.6l/min flow rate

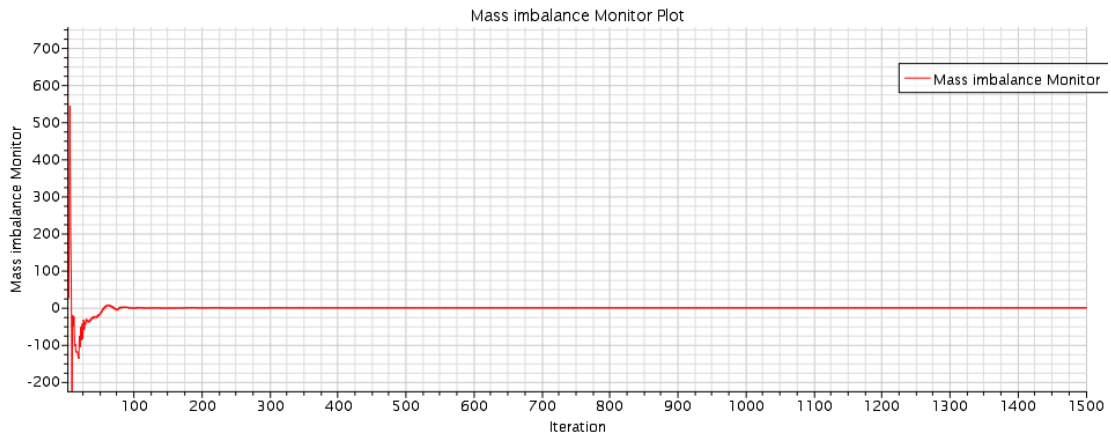


Figure 67 Mass imbalance of model 1

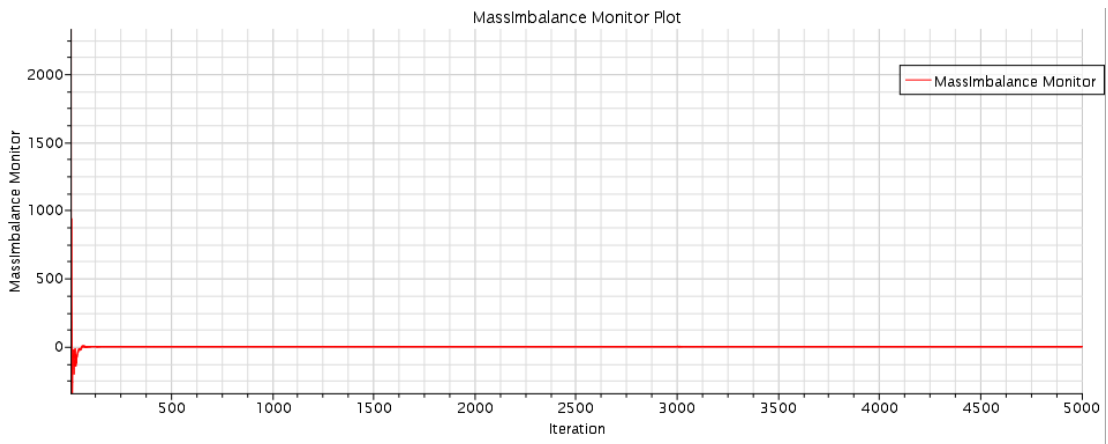


Figure 68 Mass imbalance of model 2, 13.6 l/min flow rate

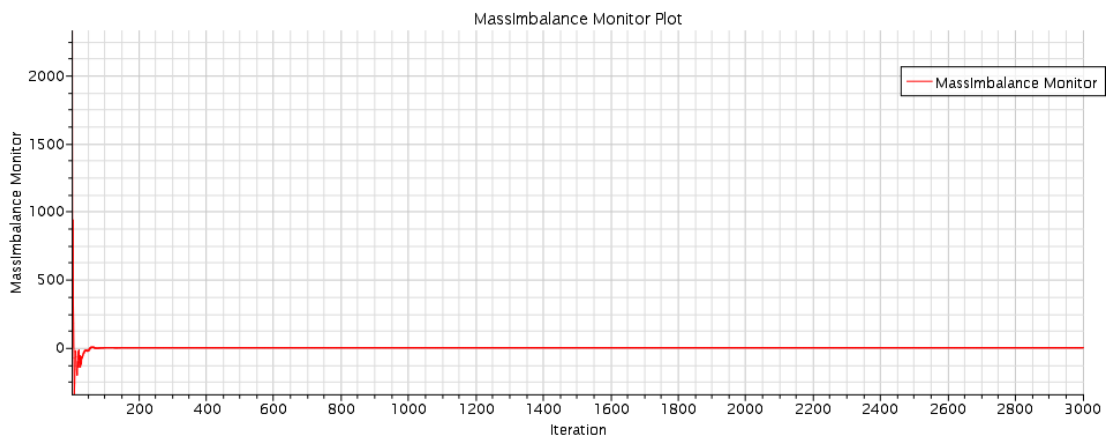


Figure 69 Mass imbalance of model 2, 18 l/min flow rate

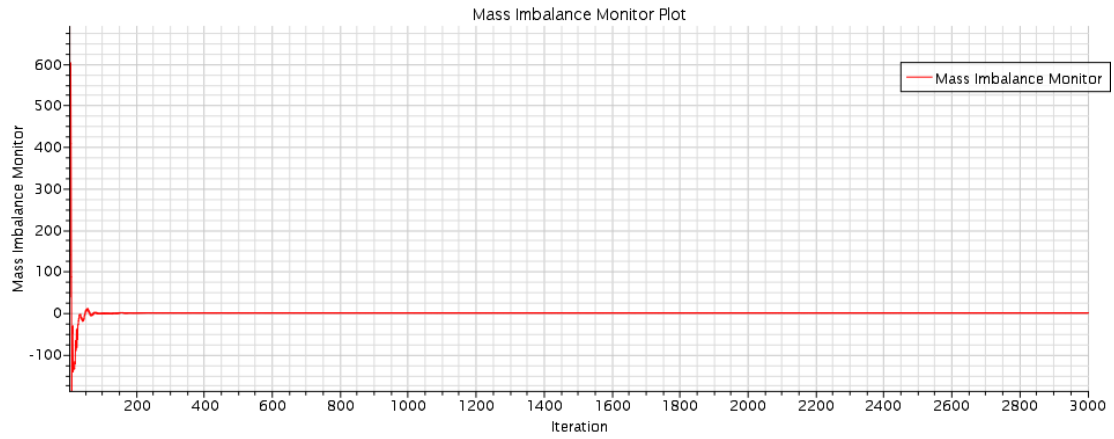


Figure 70 Mass imbalance of model 3

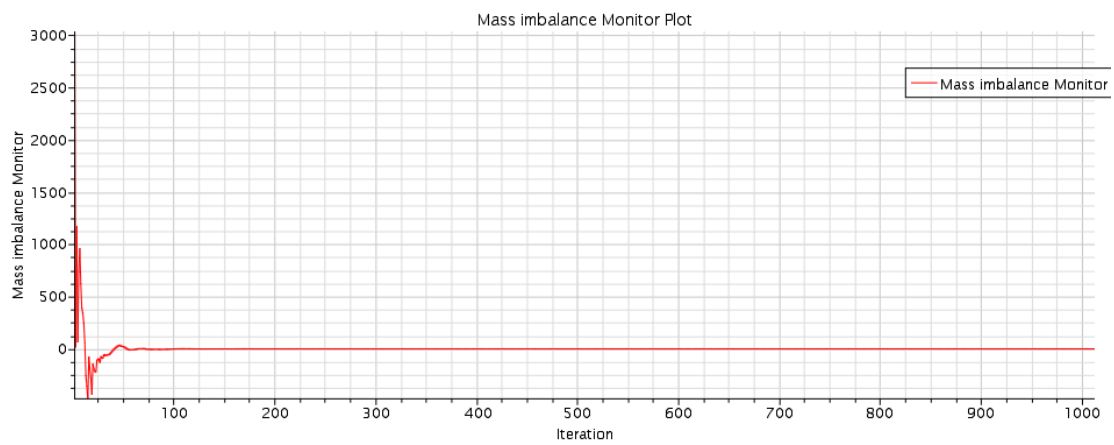


Figure 71 Mass imbalance of model 4, 13.6l/min flow rate

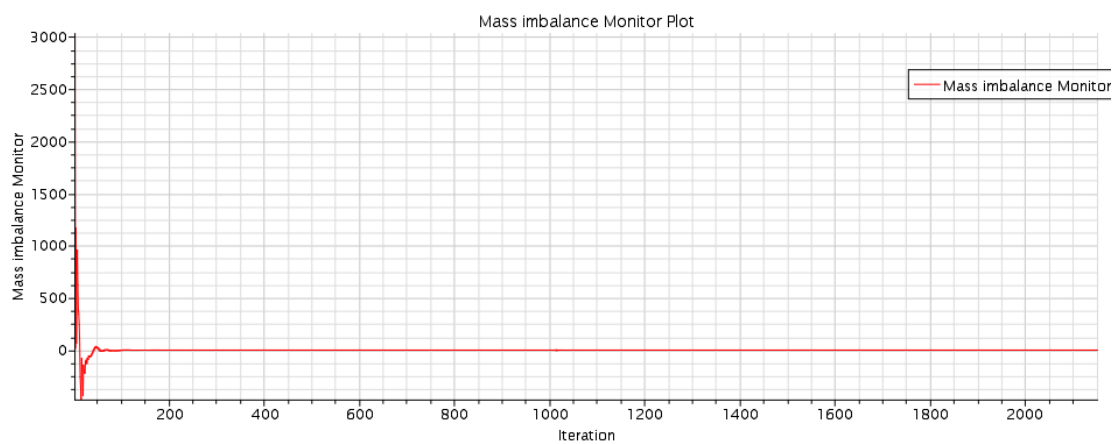


Figure 72 Mass imbalance of model 4, 18l/min flow rate

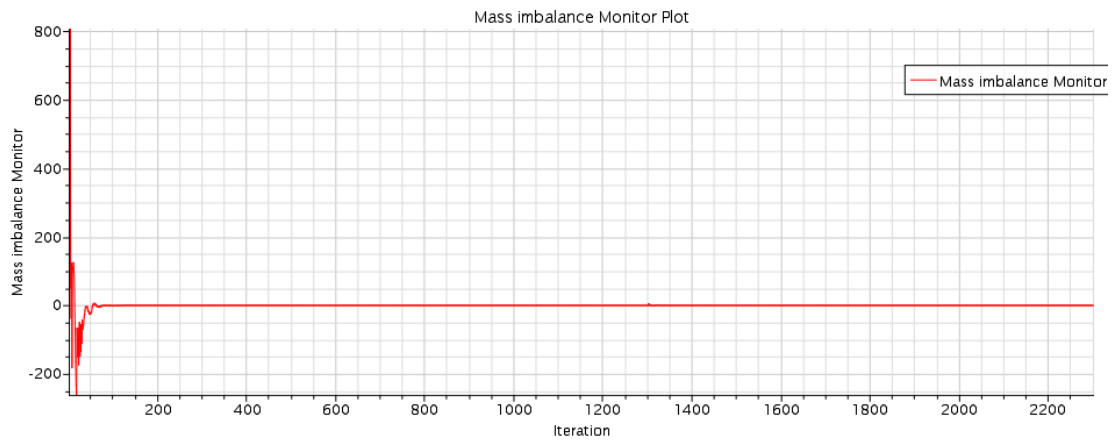


Figure 73 Mass imbalance of original model 13.6l/min flow rate

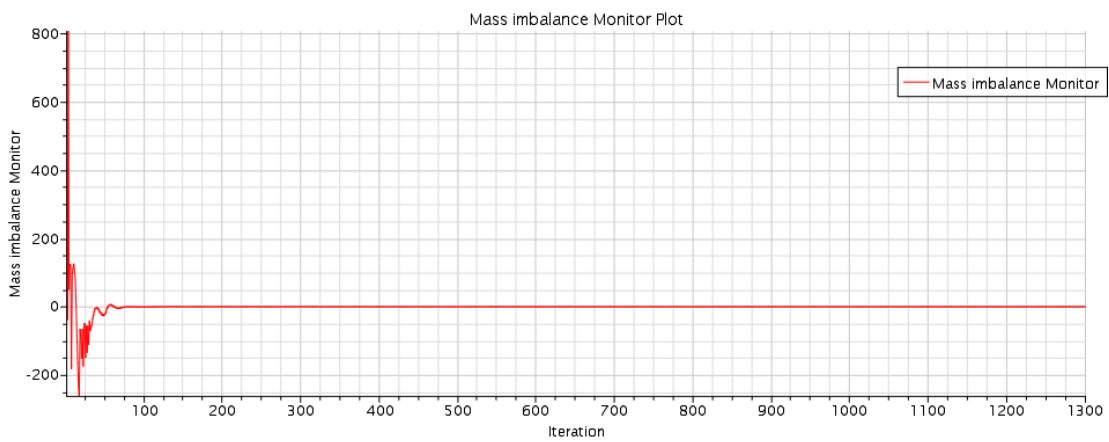


Figure 74 Mass imbalance of original model 18l/min flow rate

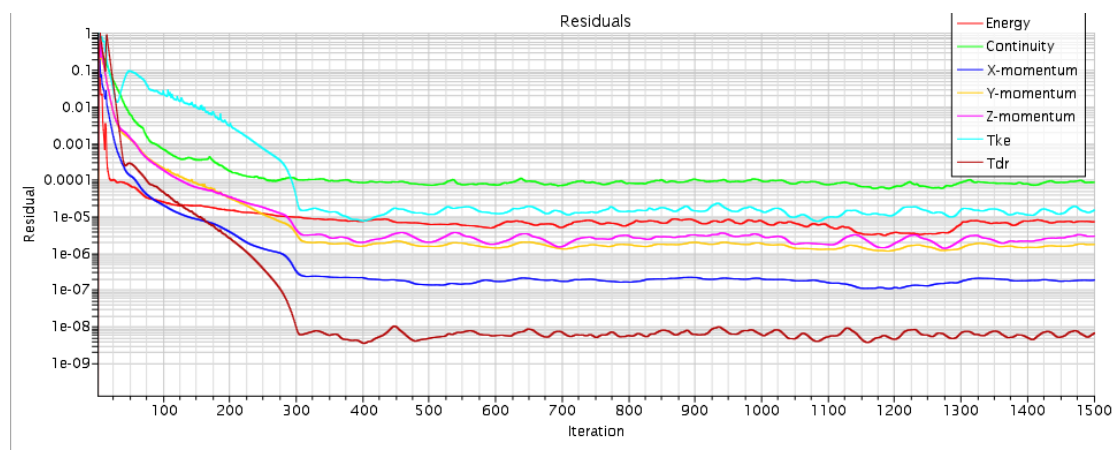


Figure 75 Residuals of model 1

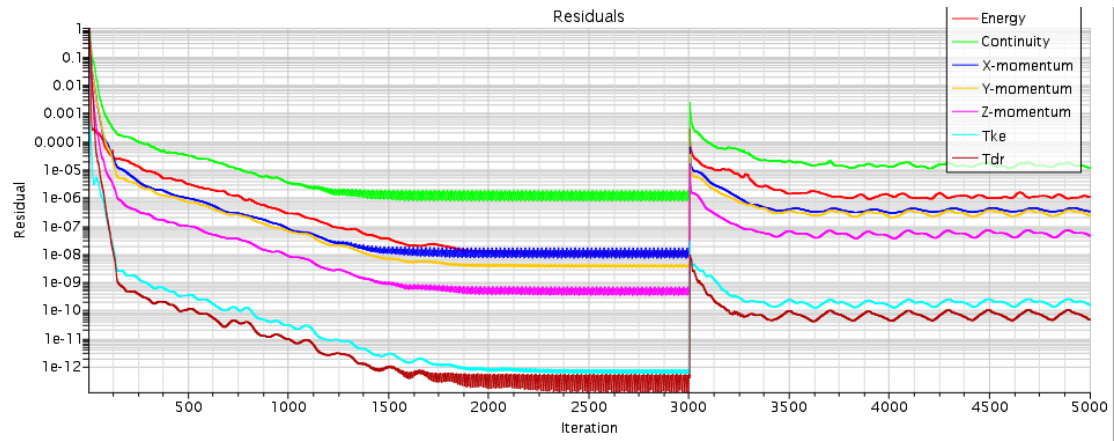


Figure 76 Residuals of model 2, 13.6l/min flow rate

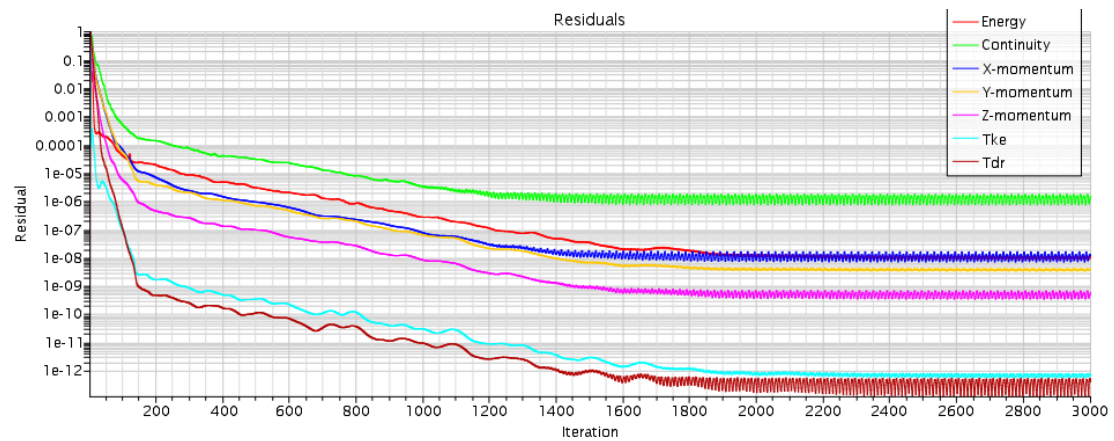


Figure 77 Residuals of model 2, 18l.min flow rate

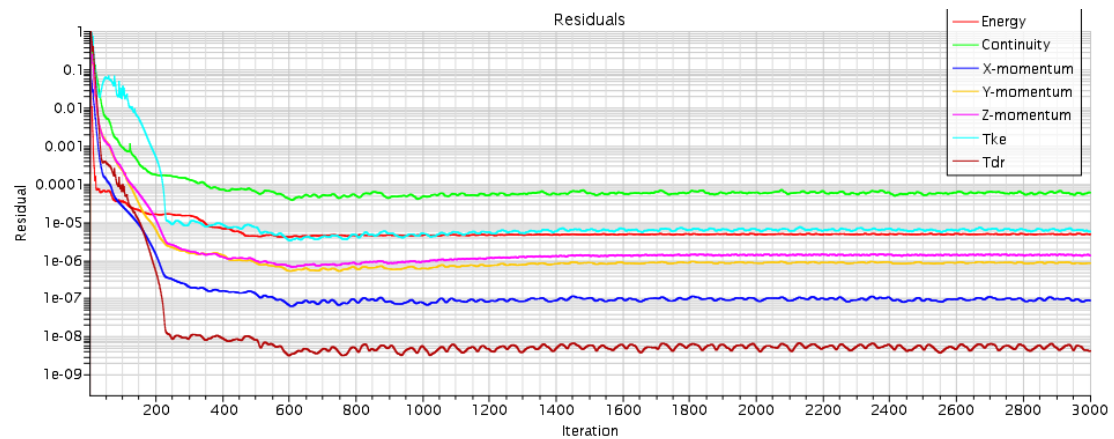


Figure 78 Residuals of model 3

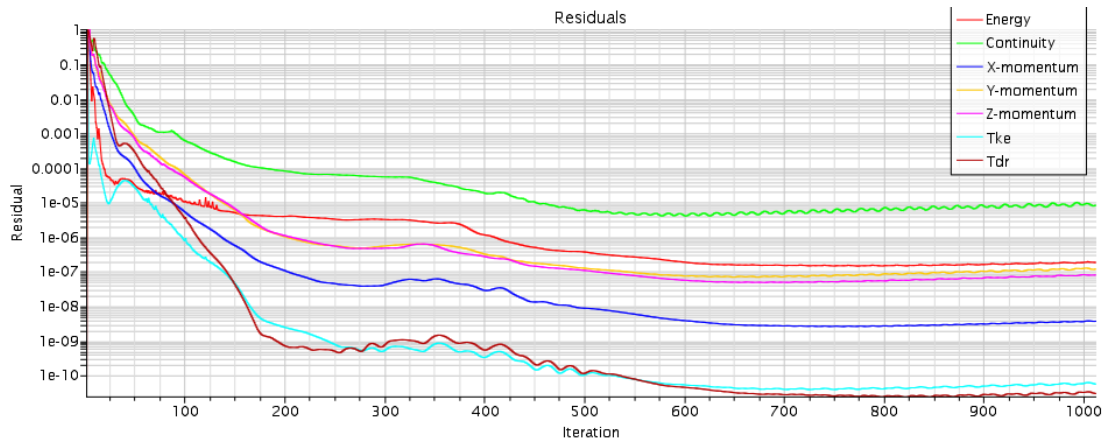


Figure 79 Residuals of model 4, 13.6l/min

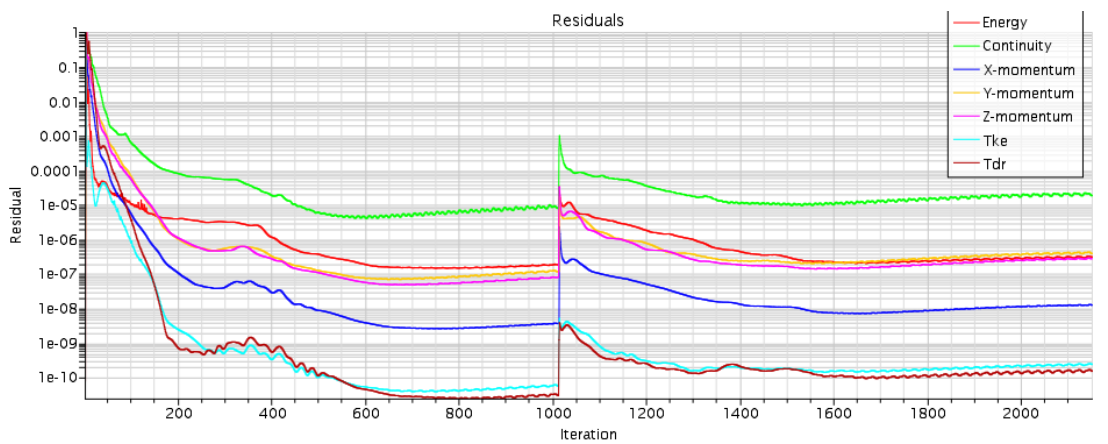


Figure 80 Residuals of model 4, 18l/min flow rate

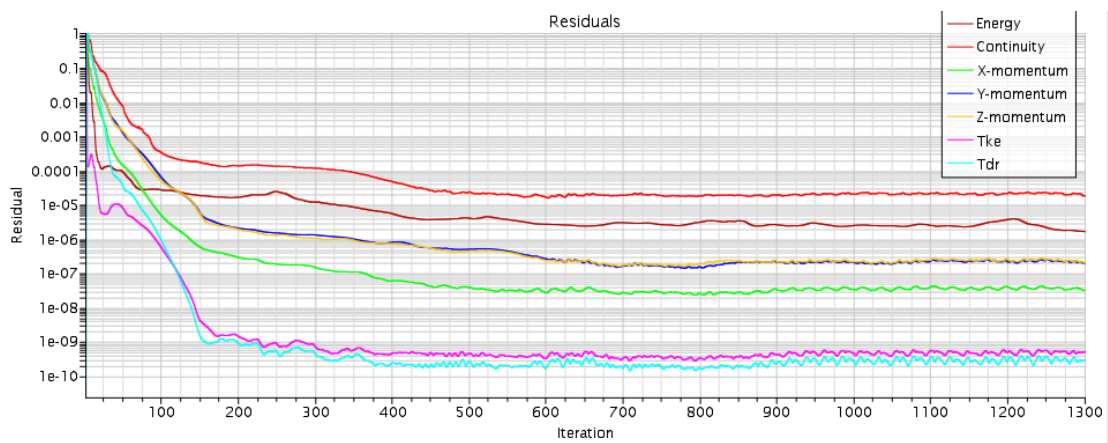


Figure 81 Residuals of original model, 18l/min flow rate

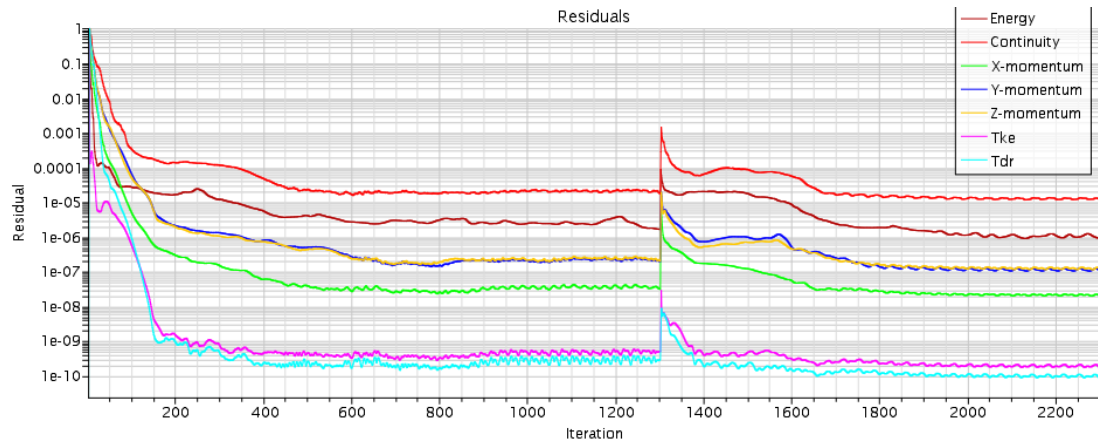


Figure 82 Residuals of original model, 13.6l/min flow rate